

Coded Aperture Mask and collimator for the CZT detector array of ASTROSAT

Some Technical Details

Sushila R. Mishra & A. R. Rao

Astronomy & Astrophysics Group, Tata Institute of Fundamental Research, Mumbai 400 007

Dipankar Bhattacharya

Astronomy & Astrophysics Group, Raman Research Institute, Bangalore 560 080

(November 2003)

1 Introduction

The Indian Multi-wavelength Satellite, *Astrosat*, has been proposed with broad-band X-ray spectroscopy in the energy range of 0.3 - 100 keV as one of its major objectives. Several of the problems dogging the field of hard X-ray continuum spectroscopy like background measurement, limited energy bandwidth, limited degrees of freedom for spectral fitting due to poor energy resolution can be effectively tackled by incorporating the new generation near-room-temperature solid state devices like Cadmium Zinc Telluride (CZT) detector arrays. It is proposed that a large area (1000 cm²) CZT detector will be developed for inclusion in *Astrosat*. These detectors have very good detection efficiency (close to 100% up to 100 keV) and have a superior energy resolution (~3% at 60 keV) compared to scintillation and proportional counters. Their small pixel size also facilitates medium resolution imaging in hard X-rays.

2 Scientific Objectives

The CZT array with its superior energy resolution (about 10% at 6 keV and 3% at 60 keV) will carry out spectral measurements (in conjunction with the SXT and the LAXPC detectors) in the 2-100 keV band with an accuracy which will be unmatched by any existing or planned mission in the 2005 time frame.

The CZT detector array will have the merit of

- (a) measuring the contribution of the non-cosmic X-ray background from 5 keV to 100 keV, simultaneously with the source intensity measurements,
- (b) enable a simultaneous spectral fit to the X-ray spectra so as to get a measure of systematic errors in the data, and
- (c) allow us to measure the contribution from confusing neighboring sources.

With its large area and sensitivity to gamma-rays, the CZT detector array can also act as an omni-directional gamma ray detector and can give important information on (a) gamma-ray bursts and (b) diffuse cosmic X-ray and gamma-ray background.

3 Detector specifications

Proportional counters and scintillating crystals are the commonly used hard X-ray detectors in X-ray astronomy. Though they can be made in large areas, they have poor energy resolution. The typical energy resolution possible in such detectors are shown in Figure 1, along with the resolution possible with the near room temperature solid state detector CZT. The improved energy resolution, particularly at higher energies, and better detection efficiency of the CZT detectors are evident from the figure.

To optimally utilize the imaging and spectroscopic characteristic of CZT detectors a 1000 cm² detector with a pixel size of 2.5 mm × 2.5 mm is planned. The salient features of the telescope is given in Table 1. The detector plane will be pixelated and to exploit this property

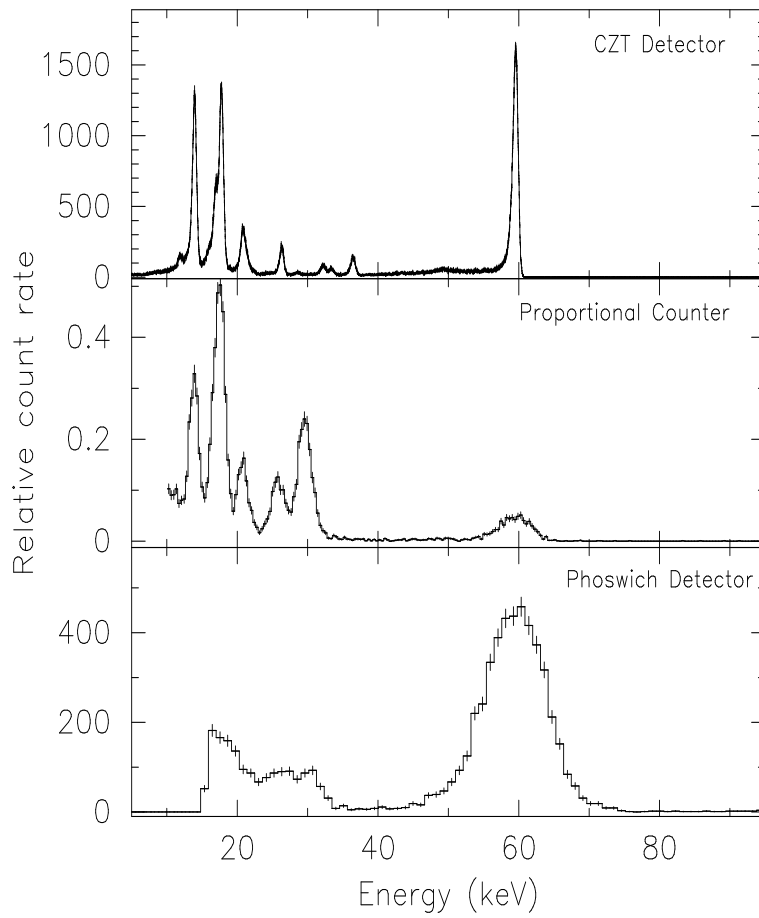


Figure 1: X-ray spectrum using various detectors for ^{241}Am radio-active source

Table 1: Details of CZT array detector

Total area	: 1024 cm ²
Number of pixels	: 16384
Pixel size	: 2.5 mm × 2.5 mm
	: (5 mm thick)
Read-out system	: ASIC based
	: (128 chips of 128 channels)
Imaging method	: Coded Aperture Mask (CAM)
size	: 1024 cm ²
element size	: 2.5 mm × 2.5 mm
material	: Tantalum
thickness	: 0.5 mm
Field of view	: 6° × 6° (25 – 100 keV)
	: 6° × 1° (5 – 25 keV)
Angular resolution	: 8'
Energy resolution	: 3% at 60 keV
Detection efficiency	: 100% in 5 – 100 keV band
Sensitivity	: 5 σ detection of 0.5 mCrab
	: source in 10 ⁴ s

a Coded Aperture Mask will define the field of view. The purpose of the mask is primarily to remove source confusion and to simultaneously measure the background contribution. The field of view is energy dependent to effectively reduce the cosmic diffuse X-ray background. A one inch thick CsI crystal will be used in an anti-coincidence mode to reject Compton-scattered background from gamma-rays. The detectors would be used in a spectroscopic mode in the energy range of 5 – 100 keV and above this energies the detectors would be operating as a all-sky gamma-ray detector with very limited imaging capability.

4 Design of CAM and collimator for CZT detector array

The CZT detector plane of (nominal) size $32\text{cm} \times 32\text{cm}$ would be made out of 64 units of 16cm^2 detectors, assembled in four quadrants. Each quadrant is equally divided into 16 units. Therefore for all the four quadrants we have, 16×4 equals 64 (2^6) units.

The single unit of (nominal) size $4\text{cm} \times 4\text{cm}$ would be made out of 256 units, i.e., single unit divided into 16×16 equals 256 pixels.

Therefore,

$$\text{Total number of pixels} = 256 \times 64 = 16384.$$

$$\text{Detector area} = 32\text{cm} \times 32\text{cm} = 1024\text{cm}^2$$

Therefore,

$$\text{Area of each pixel} = \frac{\text{Detector Area}}{\text{total no. of pixels}} = \frac{32\text{cm} \times 32\text{cm}}{16384} = 0.0625\text{cm}^2$$

$$\text{Width of each pixel} = \sqrt{0.0625\text{cm}^2} = 0.25\text{cm} = 2.5\text{mm}$$

Therefore,

$$\text{Pixel size} = 2.5\text{mm} \times 2.5\text{mm}$$

Two passive collimators of FOV (field of view) $6^\circ \times 1^\circ$ and $6^\circ \times 6^\circ$ are mounted above the detector plane. A coded aperture mask of element size $2.5\text{mm} \times 2.5\text{mm}$ made of Tantalum (thickness 0.5mm) is kept 50cm above the detector plane.

To design $6^\circ \times 1^\circ$ FOV, material used is Al as it blocks 90% X-rays and only vertical incidence on the detector plane is allowed. The thickness of the material can be calculated. Consider single unit and collimator placed above this. A single unit has 256 pixels on the detector plane but that of the collimator is divided into 8 parts i.e. between two aluminium foil there is a separation of 5mm. At 0° incidence all the area is exposed. The maximum angle (θ_o) is calculated as follows

$$\text{Angle } (\theta_o) = \tan^{-1} \left(\frac{a}{l} \right) \approx \frac{a}{l} \dots (\text{for small angle})$$

Where,

$$l = \text{height of the collimator} = 40\text{cm}$$

$$a = \text{separation} = 0.5\text{cm width for } 6^\circ \times 1^\circ \text{ FOV}$$

Therefore,

$$\frac{t_e}{t} = \frac{l}{2a} \quad (1)$$

$$t_e = t \times \frac{l}{2a} \quad (2)$$

X-ray detectors are individual photon counting device. Let N_i represent number of photons incident and N_t represent number of photons transmitted through effective thickness (t_e) we get,

$$N_t = N_i \exp(-\mu \times t_e) \quad (3)$$

where, $\mu \Rightarrow$ absorption co-efficient

$$N_t = N_i \exp \left[- \left(\frac{\mu}{\rho} \right) \times \rho \times t_e \right] \quad (4)$$

$$\frac{N_t}{N_i} = \exp \left[- \left(\frac{\mu}{\rho} \right) \times \rho \times t_e \right] \quad (5)$$

The absorption co-efficients for various materials are obtained from

<http://physics.nist.gov/PhysRefData/>

For aluminium, for 20 keV (μ/ρ) is $3.24 \text{ cm}^2/\text{gm}$, density (ρ) is $2.7 \text{ gm}/\text{cm}^3$ and (N_t/N_i) is 0.1. Therefore, the thickness (t) of the material can be calculated. The estimated thickness of the aluminium foil for $6^\circ \times 1^\circ$ FOV is 0.1mm.

Similarly, for $6^\circ \times 6^\circ$ FOV, material used is tantalum and the thickness can be calculated. Note for tantalum, separation (a) is 4cm width.

$$\Rightarrow \text{Angle } (\theta_o) = \tan^{-1} \left(\frac{4}{40} \right) = 5.7^\circ$$

Therefore, a large tube of size 4cm, material used is tantalum (thickness 0.2mm) in the energy range of 25 - 100 keV and the smaller tube of aluminium is transparent for the large tube.

Background count rates due to cosmic diffuse X-ray background (CDXRB) is shown in Table 2. The spectral form of this radiation can be adequately represented by the expression (Schonfelder et al., 1980; Mandrov et al., 1979):

$$dN(E) = 87.4E^{-2.3}dE \quad \text{photons } \text{cm}^{-2}\text{s}^{-1}\text{keV}^{-1}\text{sr}^{-1} \quad (6)$$

The representation of the spectral emission, given by equation (6), has been used to estimate the contribution of the cosmic diffuse flux to the background level of a detector (refer Space Science Reviews 57: 109 - 186, 1991).

Flux is calculated for various energy range using equation (6). For example, to calculate flux for energy range 4 - 13 keV, integrating equation (6), we get

$$\text{Flux} = 8.7 \quad \text{photons } \text{cm}^{-2}\text{s}^{-1}\text{sr}^{-1} \quad (7)$$

Counts for opening angle 1° , 2° , 5° , 10° and 60° can be obtained as shown below.

$$\text{counts/sec} = \text{Flux} \times \text{Solid Angle} \times \text{Size} \quad (8)$$

Where, solid angle (Ω) = $2\pi (1 - \cos \theta)$ steradian and θ is the opening angle.

Note : 40,000 square degree = 4π steradian

Consider, energy range from 5 - 100 keV, the total counts for opening angle $1^\circ \times 6^\circ$ is 7.672 counts/sec and that of $6^\circ \times 6^\circ$ is 46.03 counts/sec [refer table 3].

This shows that background counts for $6^\circ \times 6^\circ$ is more. To reduce the background count, $1^\circ \times 6^\circ$ collimator is used between the energy range 5 - 25 keV and $6^\circ \times 6^\circ$ collimator is used between the energy range 25 - 100 keV. This implies the total counts for opening angle $1^\circ \times 6^\circ$ is 7 counts/sec and that of $6^\circ \times 6^\circ$ is 5 counts/sec. Hence the combination of $1^\circ \times 6^\circ$ and $6^\circ \times 6^\circ$ collimator gives 12 counts/sec i.e. below 25 keV $1^\circ \times 6^\circ$ illumination on the detector plane and above 25 keV to 100 keV, $6^\circ \times 6^\circ$ illumination on the detector plane.

4.1 Geometric Description

The CZT detector is placed on the card. The design of one of the quadrant of the card is shown in Figure 2.

Table 2: Background Count rates due to CDXRB

Energy range		Flux $\text{cm}^{-2} \text{s}^{-1} \text{str}^{-1}$	Counts for opening angle				
E1 keV	E2 keV		1°	2°	5°	10°	π str
4.	13.	8.700	4.162	16.650	104.007	415.236	13665.96
13.	25.	1.372	0.656	2.626	16.402	65.483	2155.14
25.	40.	0.468	0.224	0.896	5.595	22.337	735.13
40.	100.	0.387	0.185	0.741	4.627	18.471	607.90
100.	150.	0.069	0.033	0.132	0.827	3.303	108.70
150.	200.	0.031	0.015	0.060	0.372	1.484	48.85
200.	300.	0.028	0.013	0.054	0.336	1.341	44.14
300.	400.	0.013	0.006	0.024	0.151	0.601	19.79
400.	500.	0.007	0.003	0.013	0.084	0.335	11.03
500.	600.	0.004	0.002	0.008	0.053	0.210	6.91
600.	800.	0.005	0.003	0.010	0.061	0.245	8.06
800.	1000.	0.003	0.001	0.006	0.034	0.136	4.48

Table 3: Background Count rates due to CDXRB

Energy range		Flux $\text{cm}^{-2} \text{s}^{-1} \text{str}^{-1}$	Counts for opening angle	
E1 keV	E2 keV		1° × 6°	6° × 6°
5.	10.	4.93	4.646	—
10.	25.	2.35	2.215	—
25.	50.	0.61	—	3.449
50.	100.	0.25	—	1.414

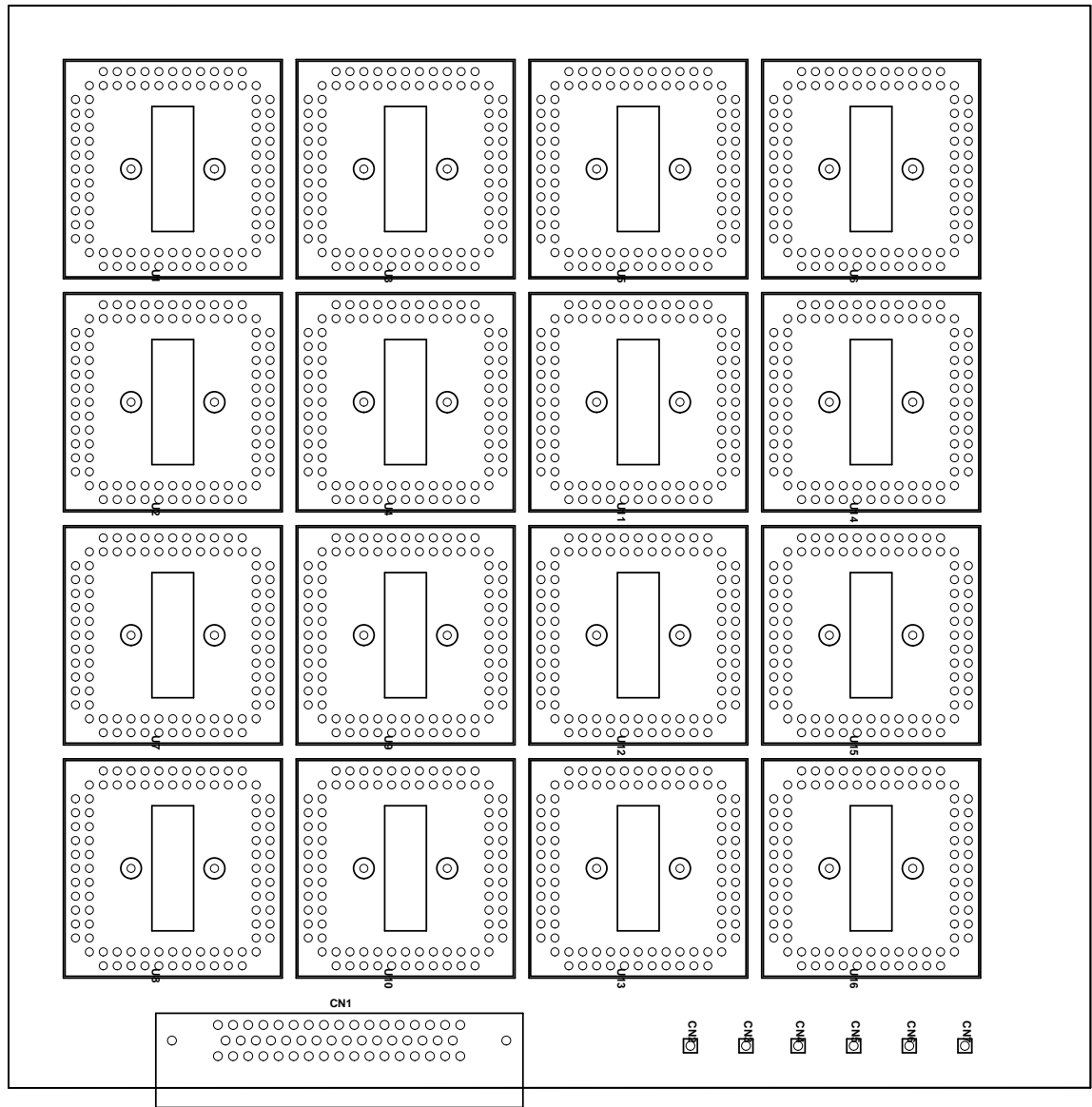


Figure 2: Design of the card i.e Chip On Board [single quadrant of nominal size 16cm × 16cm]. 2.5mm gap between unit to unit i.e. one pixel width.

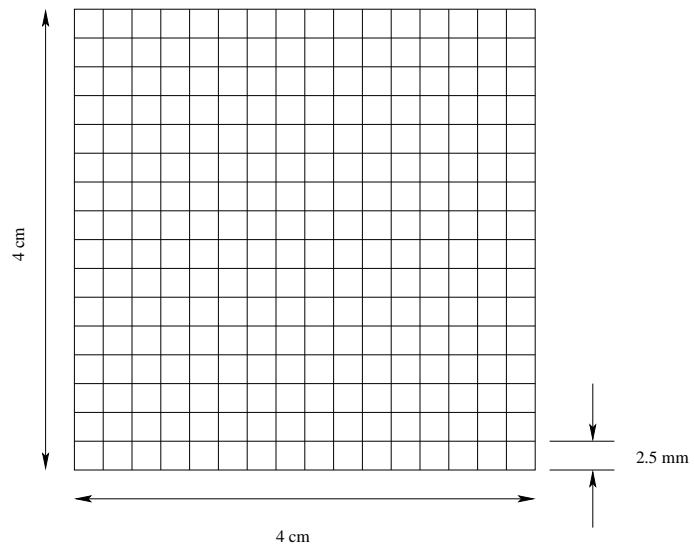


Figure 3: A single unit of the detector plane.

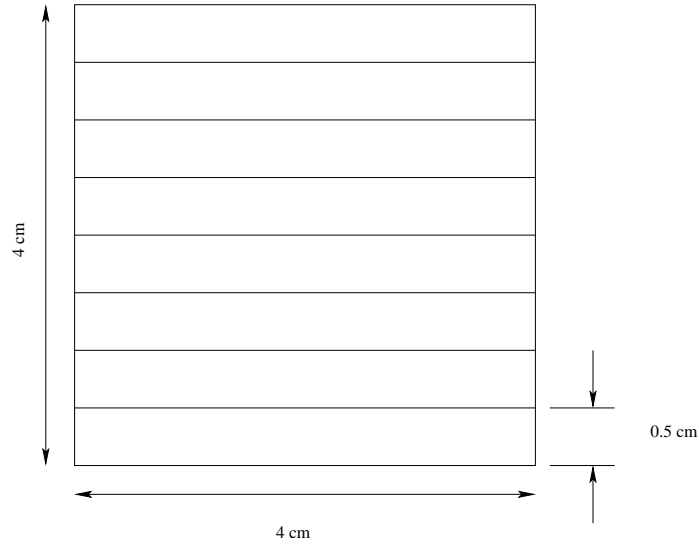


Figure 4: A single unit of the collimator.

The single unit is of size $4\text{cm} \times 4\text{cm}$ is divided into 16×16 equals 256 pixels. Each pixel is of size $2.5\text{mm} \times 2.5\text{mm}$ as shown in Figure 3. The collimator of height 40cm is placed at a gap of 10cm above the detector plane for scientific reasons. A source will be kept at one of the edge at a height of 10cm above the detector plane, to maintain flexibility of various other things on the detector.

Collimator is designed for $1^\circ \times 6^\circ$ FOV and $6^\circ \times 6^\circ$ FOV. Consider single unit of the collimator of size $4\text{cm} \times 4\text{cm}$, all the four sides is covered by a tantalum sheet of thickness 0.2mm and height 40cm [for $6^\circ \times 6^\circ$ FOV].

Each single unit is further divided into 8 parts horizontally (as shown in Figure 4) by a aluminium sheet of thickness 0.1mm and height 40cm in one of the quadrant [for $1^\circ \times 6^\circ$].

The quadrant next to it will have a vertical division, thus there will be alternate horizontal and vertical division from quadrant to quadrant.

2.5mm gap is maintained between unit to unit and 2cm gap between quadrant to quadrant, for flexibility of various other things on the detector.

Each rectangle is of size $4\text{cm} \times 0.5\text{cm}$ and the distance between two aluminium sheet is 5mm. There are 32 pixels in one rectangle of size $40\text{mm} \times 5\text{mm}$.

4.2 Efficiency of the detector as a function of energy

$$\text{Efficiency}(E) = 1 - \exp\left[-\left(\frac{\mu}{\rho}\right) \times \rho \times t\right] \quad (9)$$

Where, μ is the absorption co-efficient, ρ is the density of the material and t is the thickness of the material in cm.

Absorption coefficient of various materials.

Data is obtained from:

<http://physics.nist.gov/PhysRefData/>

The following data files are enclosed:

xcom3_Al.txt	xcom3_BGO.txt	xcom3_cop.txt
xcom3_CsI.txt	xcom3_CZT.txt	xcom3_lead.txt
xcom3_NaI.txt	xcom3_Si.txt	xcom3_Tung.txt

These files can be read using the FORTRAN code:

```
abs_read.f      Executable file:  a.out*
                  Output file    absco.out
(program requires a list of input files given in : fil)
```

The FORTRAN code abs_read.f calculates the absorption(%) due to photoelectric, Compton and total.

The content of input file fil contains the following :

```
xcom3_Al.txt
Teflon.dat
xcom_mylar.txt
xcom3_BGO.txt
xcom3_cop.txt
xcom3_CsI.txt
xcom3_CZT.txt
xcom3_lead.txt
xcom3_NaI.txt
xcom3_Si.txt
xcom3_Tung.txt
```

Teflon.dat
xcom3_Delrin.txt

The code will ask the user to select any of the above mentioned file. For example xcom3_CZT.txt file is selected. Also, the code will ask the user to enter the thickness in cm for CZT with density 5.9.

The content of the file xcom3_CZT.txt contains the following :

12 5.9 0.5
CZT

Constituents (Atomic Number : Fraction by Weight)

Z=30 : 0.027789
Z=48 : 0.429945
Z=52 : 0.542266

Edge	Photon Energy MeV	Scattering		Photo- electric Absorp. cm2/g	Pair Production		Total Attenuation	
		Coherent cm2/g	Incoherent cm2/g		In Nuclear Field cm2/g	In Electron Field cm2/g	With Coherent Scatt. cm2/g	Without Coh. Scatt. cm2/g
	1.000E-03	7.88E+00	5.07E-03	7.77E+03	0.00E+00	0.00E+00	7.78E+03	7.77E+03
	1.003E-03	7.87E+00	5.09E-03	7.72E+03	0.00E+00	0.00E+00	7.73E+03	7.72E+03
	1.006E-03	7.87E+00	5.12E-03	7.67E+03	0.00E+00	0.00E+00	7.68E+03	7.67E+03
	1.006E-03	7.87E+00	5.12E-03	7.86E+03	0.00E+00	0.00E+00	7.87E+03	7.86E+03
	1.013E-03	7.87E+00	5.17E-03	7.74E+03	0.00E+00	0.00E+00	7.75E+03	7.74E+03
	1.020E-03	7.86E+00	5.23E-03	7.63E+03	0.00E+00	0.00E+00	7.64E+03	7.63E+03
	1.020E-03	7.86E+00	5.23E-03	7.68E+03	0.00E+00	0.00E+00	7.69E+03	7.68E+03
	1.031E-03	7.85E+00	5.32E-03	7.53E+03	0.00E+00	0.00E+00	7.54E+03	7.53E+03
	1.043E-03	7.84E+00	5.41E-03	7.40E+03	0.00E+00	0.00E+00	7.41E+03	7.40E+03
	1.043E-03	7.84E+00	5.41E-03	7.45E+03	0.00E+00	0.00E+00	7.45E+03	7.45E+03
	1.116E-03	7.78E+00	6.02E-03	6.42E+03	0.00E+00	0.00E+00	6.43E+03	6.42E+03
	1.194E-03	7.72E+00	6.68E-03	5.55E+03	0.00E+00	0.00E+00	5.55E+03	5.55E+03
	1.194E-03	7.72E+00	6.68E-03	5.57E+03	0.00E+00	0.00E+00	5.58E+03	5.57E+03
	1.500E-03	7.46E+00	9.35E-03	3.34E+03	0.00E+00	0.00E+00	3.35E+03	3.34E+03

The values of (μ/ρ) can be taken from the above file for photoelectric, Compton and total for various energy range and the efficiency can be calculated using equation (8) respectively. The

output is stored in the file absco.out, contains absorption(%) due to photoelectric, compton and total for various energy range in keV.

Content of abs_read.f

```
-----  
program abs_read  
  dimension co(7)  
  character*30 f_name  
3   continue  
  open(1,FILE='fil')  
  print*, ' Files Availabe: Choose one'  
  do i = 1,13  
  read(1, '(a)',err=10,end=10) f_name  
    write(*,300) i, f_name  
300  format(1x,i3,2x,a30)  
  enddo  
  rewind(1)  
  read*, ii  
  do i = 1, ii  
  read(1, '(a)',err=10,end=10) f_name  
*    write(*,300) i, f_name  
  enddo  
  close(1)  
  open(1,FILE=f_name)  
  read(1,*,err=10,end=10) i, rho  
  print*, i, rho  
  read(1, '(a)',err=10,end=10) f_name  
  write(*,400) rho, f_name  
400  format(1x,'Density: ',f8.2, ' Material : ',2x,a30)  
  print*, ' Give Thickness in cm '  
  read *, thick  
  rho = rho * thick  
  do j = 1, i  
  read(1,*,err=10,end=10)  
  enddo  
  open(2,FILE='absco.out')  
  print*, ' Energy in keV, absorpton (%) due to Photoelectric'  
  print*, ' Compton and Total written in File absco.out'  
  do i = 1,1000  
  read(1,*,err=10,end=10) en, co  
*    read(1,100,err=10,end=10) en, co  
100  format(6x,e9.3,1x,e8.2,2(2x,e8.2,2x),1x,3(e8.2,2x),2x,e8.2)  
    co1 = co(3)*rho
```

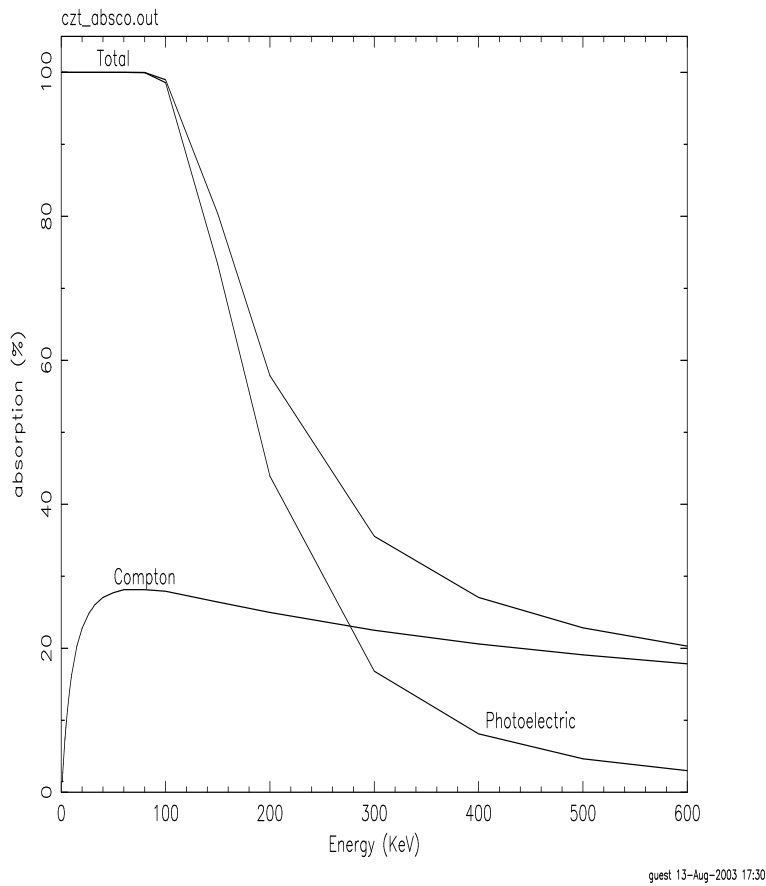


Figure 5: Efficiency of CZT Detector as a function of energy.

```

co2 = co(2)*rho
co3 = co(7)*rho
co1 = 1 - exp(-1.*co1)
co2 = 1 - exp(-1.*co2)
co3 = 1 - exp(-1.*co3)
write(2,200)en*1000,co1*100,co2*100,co3*100
*
write(*,*)en*1000,co1*500
200 format(4(2x,e14.6))
enddo
10 stop
end

```

The output file absco.out is used for plotting, energy in keV versus absorption(%) due to photoelectric, compton and total scattering.

4.3 Design of the Coded Aperture Mask (CAM)

Coded Aperture imaging aims to find the location of a source in the field of view by finding the shift, from central position, of the mask shadow cast by it on the detector (Ables 1968).

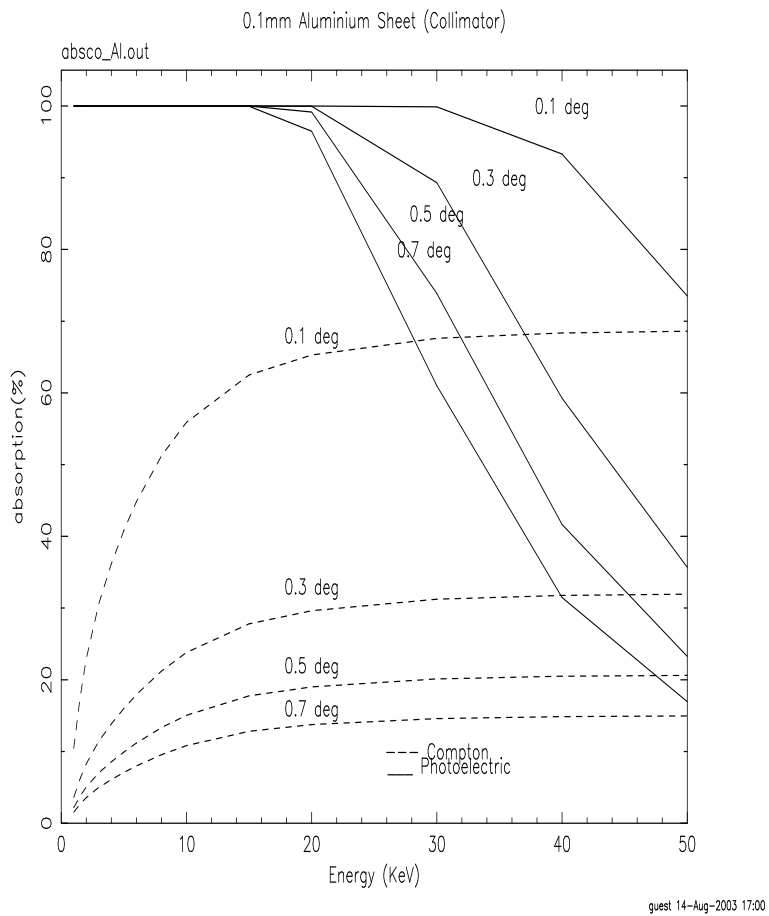


Figure 6: Efficiency of aluminium for various angle as a function of energy.

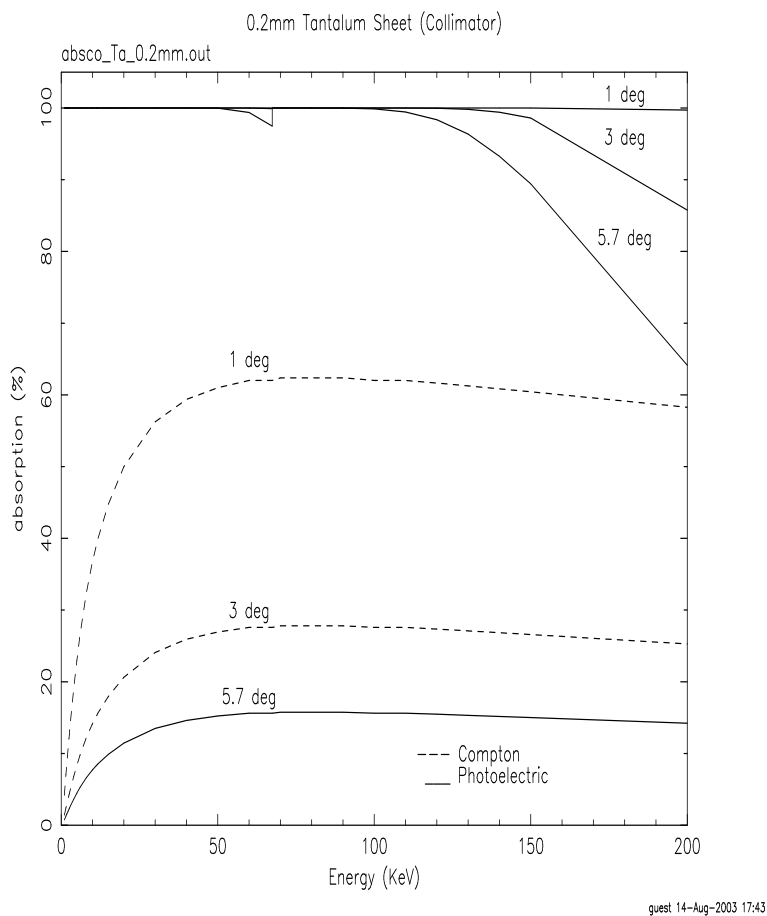


Figure 7: Efficiency of Tantalum for various angle as a function of energy.

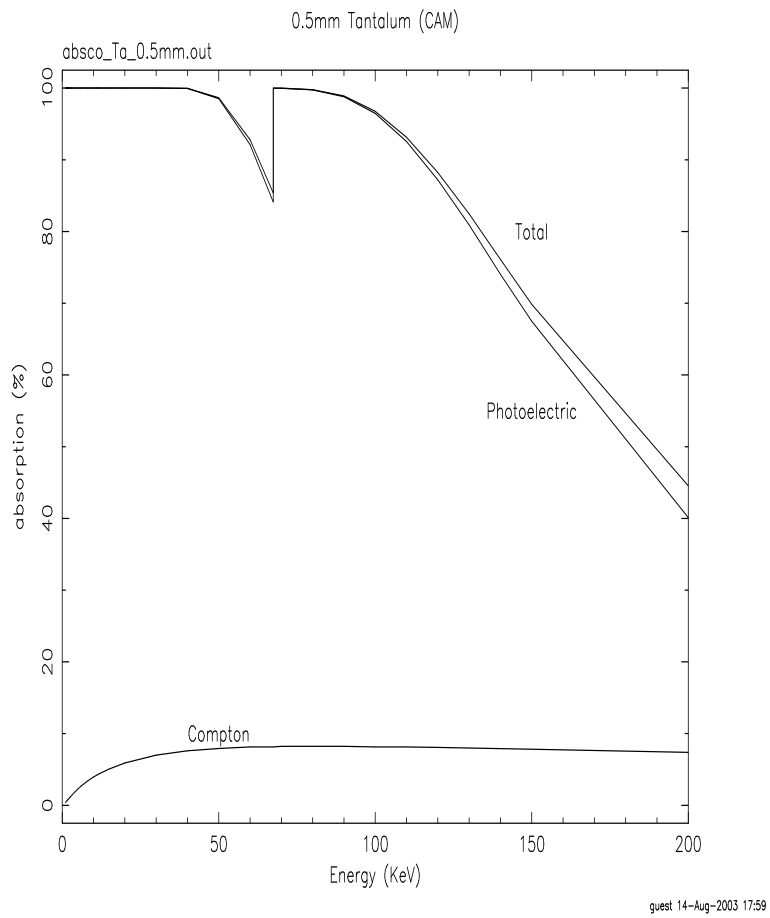


Figure 8: Efficiency of Tantalum (CAM) as a function of energy.

In practice there would be multiple sources in the field of view at any given time, so to avoid ambiguous results, it is desirable that the autocorrelation of the mask pattern has only a single peak at zero shift. It is possible to obtain this if the mask pattern is chosen to be a Uniformly Redundant Array (URA), and it is ensured that every detector element is exposed to one full mask pattern, possibly in cyclic permutation (Fenimore and Cannon 1978).

The design of the CAM for CZT detector are such that the size of the mask plate in the direction of coding is the same as that of the detector itself. In such a design (called a ‘box-type’ or ‘simple’ system) exposure to the full mask pattern is not possible anywhere except exactly at the middle of the coded field of view. At all other angles only a part of the shadow of the mask falls on the detector. This prevents the URA-property of a single peak in the response function from being realised. In the otherwise flat sidelobe pattern, undulations now appear. However among all possible patterns with the same transmission, URAs still yield peaks of minimum height in the response function, and remain the patterns of choice.

URAs are constructed out of cyclic difference sets (CDS): these are sets of integers characterized by three numbers n , k and z . A CDS, where D is a collection of k integers $\{I_1, I_2, \dots, I_k\}$ in the range $0 \leq I_i < n$, such that the congruence $I_i - I_j = J \pmod{n}$ has exactly z solution pairs (I_i, I_j) within D (Baumert 1971). A CDS can be represented as a binary sequence a_i , $0 \leq i < n$, in which an element a_i is set to 1 if i is a member of the CDS, and set to zero otherwise. In the mask pattern the 1-s of the CDS binary sequence would represent open holes, and the 0-s the closed holes. This would be called an URA pattern. Clearly, the ratio k/n would decide the transmission fraction of the URA mask.

URAs can be constructed for various levels of transmission, up to a maximum of about 50%. Usually a smaller transmission fraction is also associated with a better image definition. An extreme example would be a pin-hole camera where an excellent image definition is obtained by reducing the transmission almost to zero. One of the design requirements for the CZT mask is to obtain as much transmission as possible. Among patterns capable of doing so are the pseudo-Noise Hadamard sets which yield near-50% transparency (Caroli et al 1987, in 't Zand 1992). We have adopted this in the present context.

A pseudo-noise Hadamard set is constructed from a shift-register algorithm (Peterson 1961):
Let

$$P = \sum_{j=0}^m p_j \times x^j$$

represent a polynomial of degree m in x . From these one chooses “primitive” polynomials, for which the coefficients p_j can take values only 0 or 1. In order to keep the order intact, p_m must then always be 1. Among these primitive polynomials, one then picks “irreducible” ones, i.e. those which cannot be factorised. Such an irreducible primitive polynomial of degree m can then be used as a generating function of a mask pattern of length $n = 2^m - 1$. Let this be represented by a sequence

$$a_i, \quad i = 0, \dots, (2^m - 2)$$

where a_i are either 0 or 1, with 1-s representing open mask elements. One can choose the first m elements,

$$a_i, \quad i = 0, \dots, (m - 1)$$

arbitrarily. The following elements are then generated using the shift register algorithm

$$a_{i+m} = \sum_{j=0}^{m-1} p_j \times a_{i+j} \quad (\text{mod } 2)$$

This is the method that has been used in the generation of the CZT masks. An optimal mask design would have mask element dimensions matching the detector pixel.

The collimator design for the CZT camera essentially isolates $4\text{cm} \times 4\text{cm}$ portions of the detector array from the neighbouring ones. The CAM design is therefore carried out for one such $4\text{cm} \times 4\text{cm}$ unit, and is replicated for other such units in the camera. We recall that a single unit of size $4\text{cm} \times 4\text{cm}$ is divided into a total of 256 (16×16) pixels corresponding to $6^\circ \times 6^\circ$ FOV. For low energy photons each single unit is further divided into 8 parts, each containing 32 pixels, arranged in 16 rows and 2 columns.

The task of the mask design therefore now consists of optimizing a 16×16 mask pattern with tolerable sidelobe response, each 16×2 sub-patterns of which will also have an acceptable imaging quality.

We approach this by first generating a pseudo-noise URA, which yields 255 elements (127 closed, 128 open). In order to fit this into the required 256 element pattern we add an extra closed element, which brings the transparency of the mask to exactly 50%.

These patterns are then folded into 16×16 arrays, which are then examined for sidelobe levels. This is done at two levels. First, the 8 sub-patterns consisting of 32 elements each, corresponding to the low energy collimator, are examined through a cyclic autocorrelation and a figure of merit representing the quality of the pattern is generated. A total figure of merit for the whole pattern is obtained by summing the figure of merit values for the 8 individual sub-patterns. Patterns exhibiting the largest overall figure of merit are then examined using a 2-d autocorrelation of the full pattern and the one exhibiting the smallest local peaks above average is chosen for final implementation.

Generation of 255 element pseudo noise URAs require primitive polynomials of order 8. We use shift register algorithm to generate the 255 element patterns from all possible 8^{th} order primitive polynomials and subject them to a cyclic autocorrelation.

The Cyclic Autocorrelation Function (CACF) defined as

$$CACF(k) = \sum_{i=k}^{n-1} a_i \times a_{i-k} + \sum_{i=0}^{k-1} a_i \times a_{i-k+n}$$

Patterns showing a single peak and flat sidelobes in the cyclic autocorrelations function are chosen to be URAs. This task is performed by a code 'CAM_CACF.c' and the URAs generated are stored in the output file 'Mask.dat'.

We found that 16 URAs could be generated using this method, the corresponding 8^{th} order polynomials (generating functions) are listed in table 4

Mask Pattern	Polynomial
1	$x^8 + x^4 + x^3 + x^2 + 1$
2	$x^8 + x^5 + x^3 + x^1 + 1$
3	$x^8 + x^5 + x^3 + x^2 + 1$
4	$x^8 + x^6 + x^3 + x^2 + 1$
5	$x^8 + x^6 + x^4 + x^3 + x^2 + x^1 + 1$
6	$x^8 + x^6 + x^5 + x^1 + 1$
7	$x^8 + x^6 + x^5 + x^2 + 1$
8	$x^8 + x^6 + x^5 + x^3 + 1$
9	$x^8 + x^6 + x^5 + x^4 + 1$
10	$x^8 + x^7 + x^2 + x^1 + 1$
11	$x^8 + x^7 + x^3 + x^2 + 1$
12	$x^8 + x^7 + x^5 + x^3 + 1$
13	$x^8 + x^7 + x^6 + x^1 + 1$
14	$x^8 + x^7 + x^6 + x^3 + x^2 + x^1 + 1$
15	$x^8 + x^7 + x^6 + x^5 + x^2 + x^1 + 1$
16	$x^8 + x^7 + x^6 + x^5 + x^4 + x^2 + 1$

Table 4: Generating Functions

We then extend the resulting URA sequences by adding a single closed element(0) (stored in the file 'Mask_m8.dat'). Linear wrap into 16×16 matrices are then performed to generate the final 2-d patterns (stored in 16 different files 'LWrap[1..16]_m8.dat').

All the 16 mask patterns are shown in Figure 9.

From each of these 16 mask patterns 2×16 sub-patterns were chosen, either row-wise or column-wise, and cyclic autocorrelation was performed to assess the figure of merit, defined as

$$Figure\ of\ merit\ (FOM) = \frac{1 - a}{\delta a}$$

where a is the average and δa is the standard deviation (root mean square) of the 1-d 32 element patterns, for low-energy imaging. This task is performed by the codes 'FOMrow.c', 'FOMcol.c' and corresponding outputs are stored in the files 'FOMrow.dat' and 'FOMcol.dat'.

Figures 10 to 13 show plots of row-wise cyclic autocorrelation for the mask patterns 1 to 16. The corresponding values of figure of merit are noted in table 5. In table 6 column-wise figure of merit are also listed, and are seen to be much poorer than the row-wise sub-patterns selection. Finally to assess the quality of 2-d imaging at higher energies, linear autocorrelations defined as

$$LACF(k, m) = \sum_{i=k}^{n-1} \sum_{j=m}^{n-1} a_{i,j} \times a_{(i-k),(j-m)}$$

were performed on the full mask patterns. Plots 14 to 29 display the 3-d and contour plot, of the resulting linear autocorrelation functions.

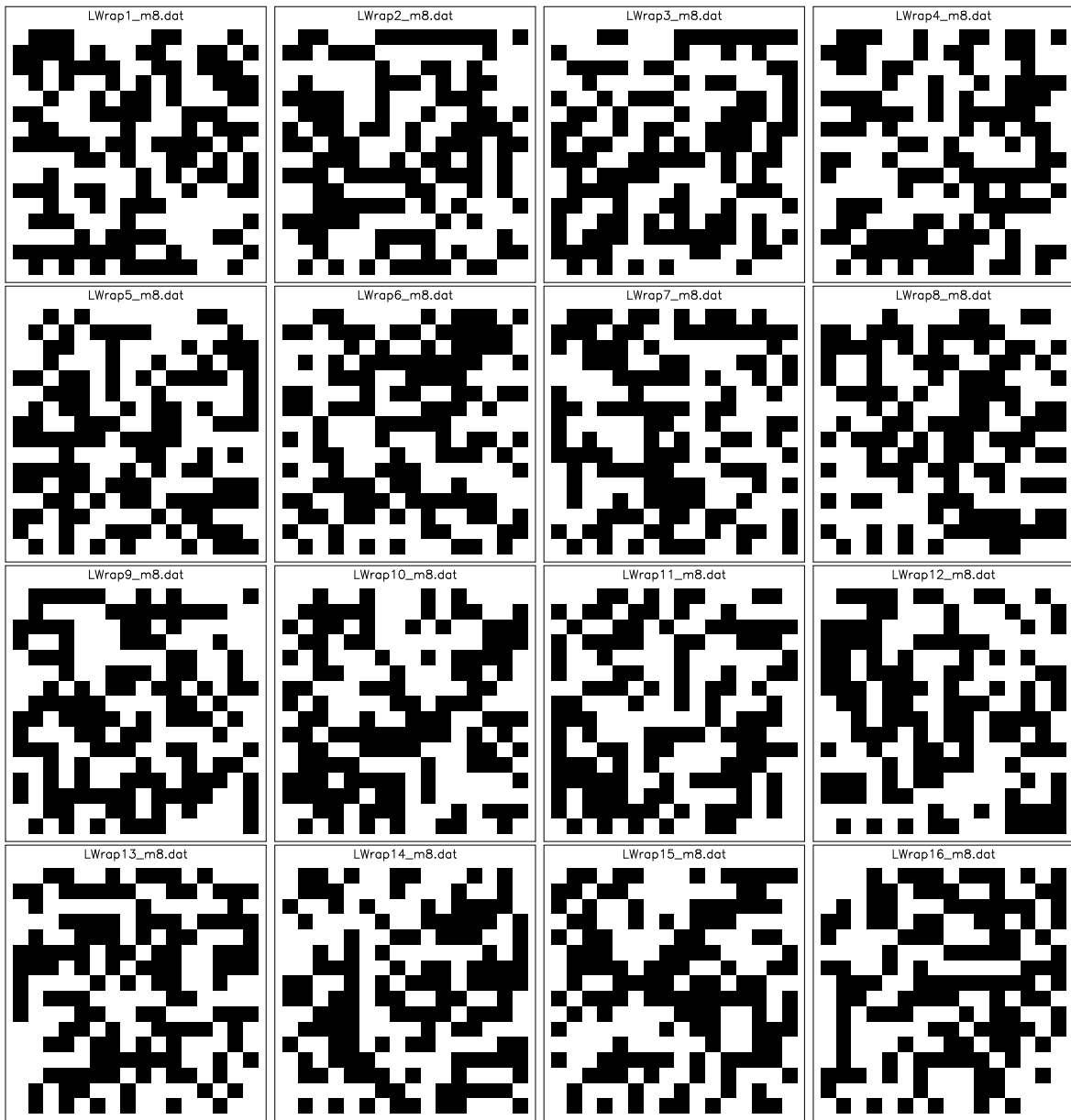


Figure 9: The Coded Aperture Mask patterns generated using 16×16 Linear Wrap

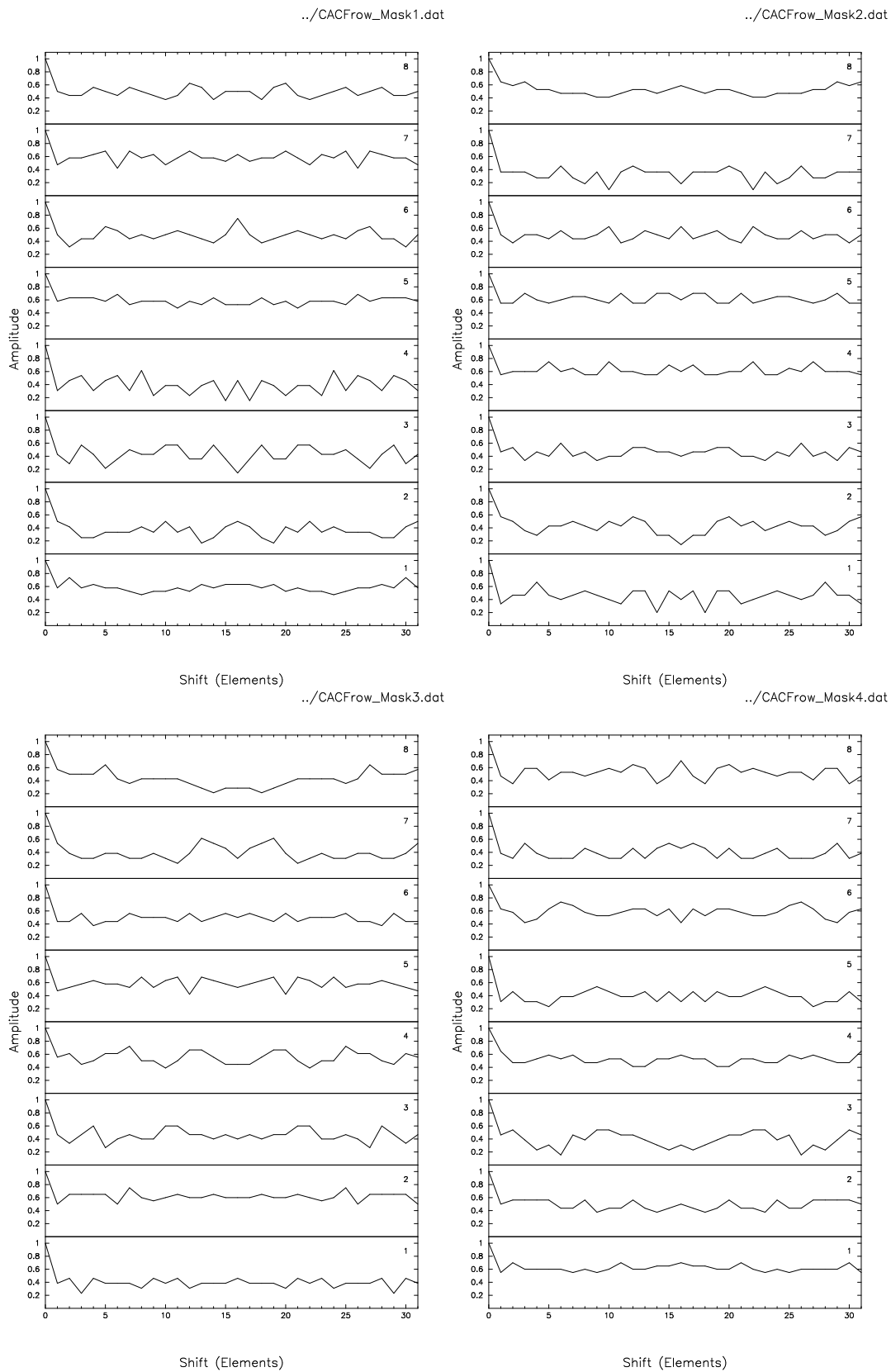


Figure 10: 1-D Cyclic autocorrelation function row-wise for mask pattern 1-4

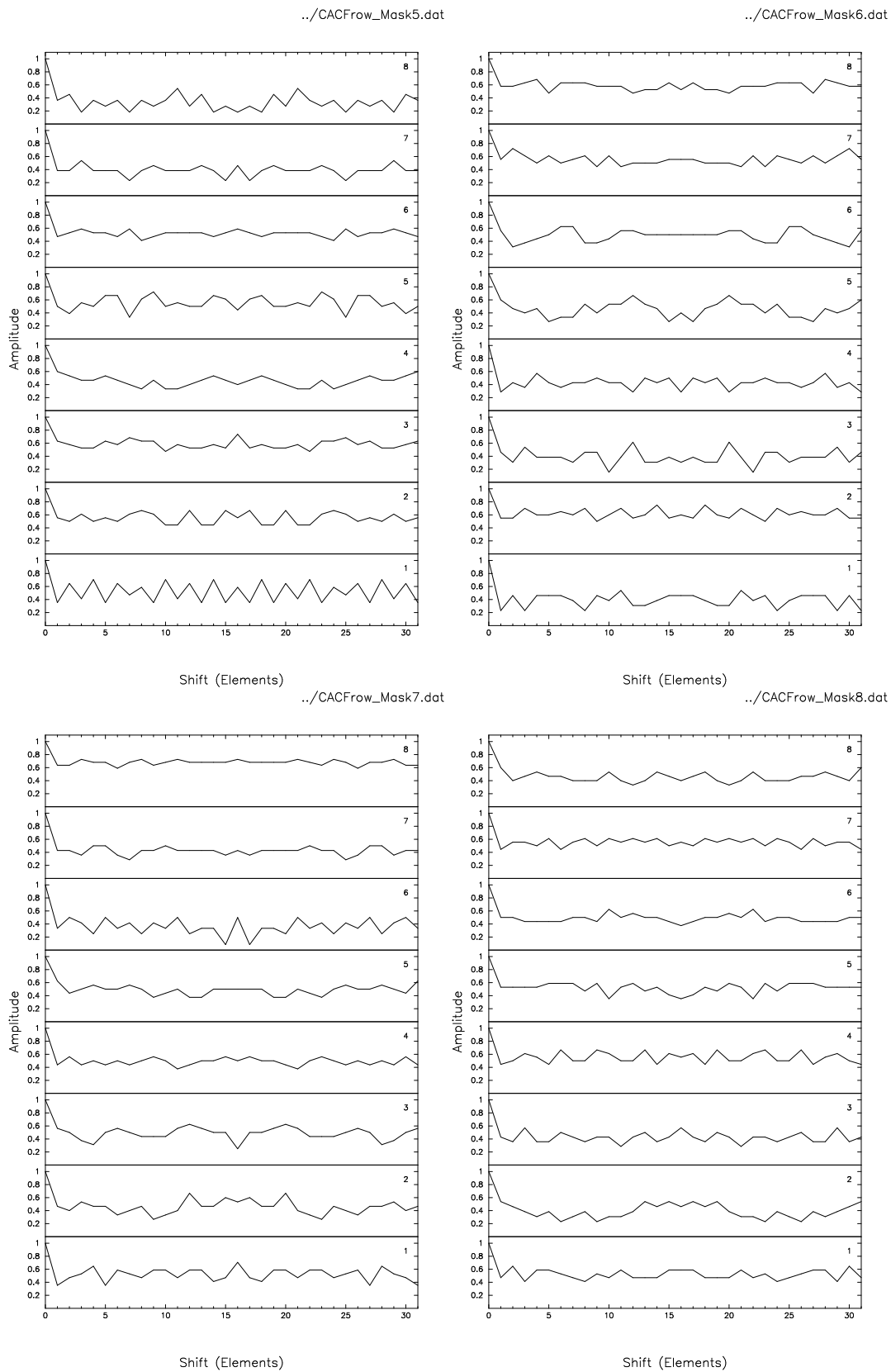
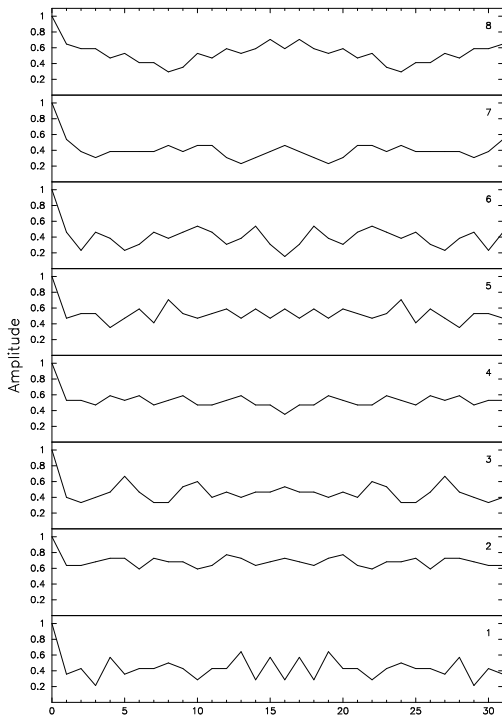


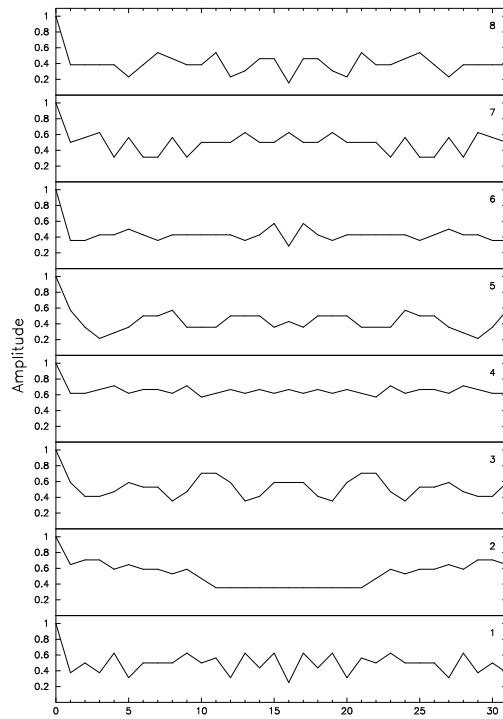
Figure 11: 1-D Cyclic autocorrelation function row-wise for mask pattern 5-8

../CACFrow_Mask9.dat



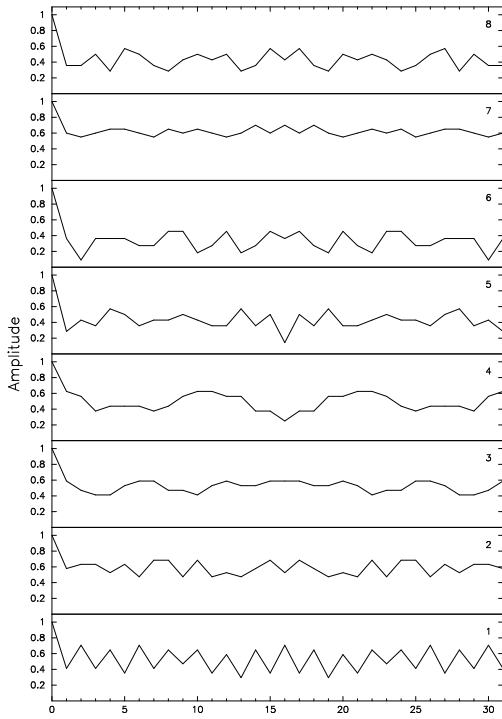
Shift (Elements)

../CACFrow_Mask10.dat



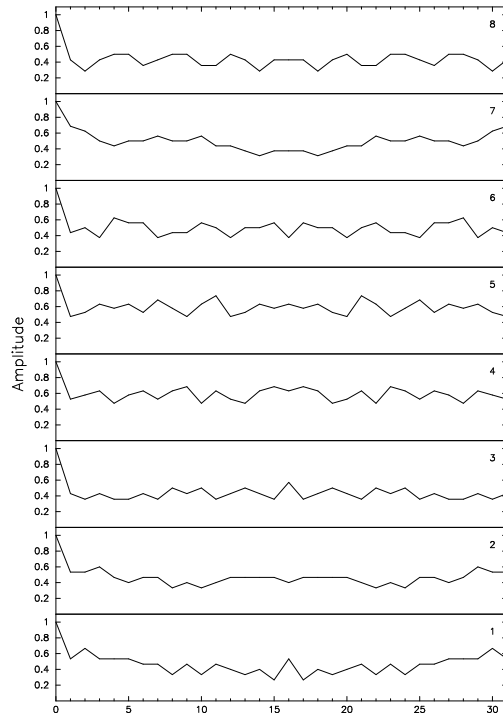
Shift (Elements)

../CACFrow_Mask11.dat



Shift (Elements)

../CACFrow_Mask12.dat

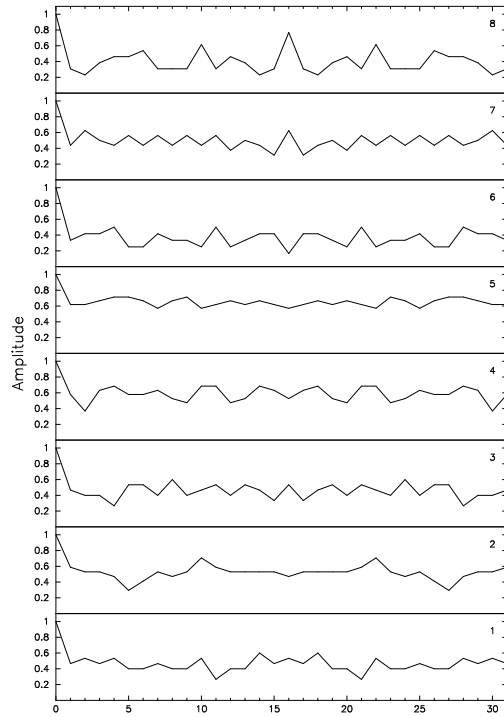
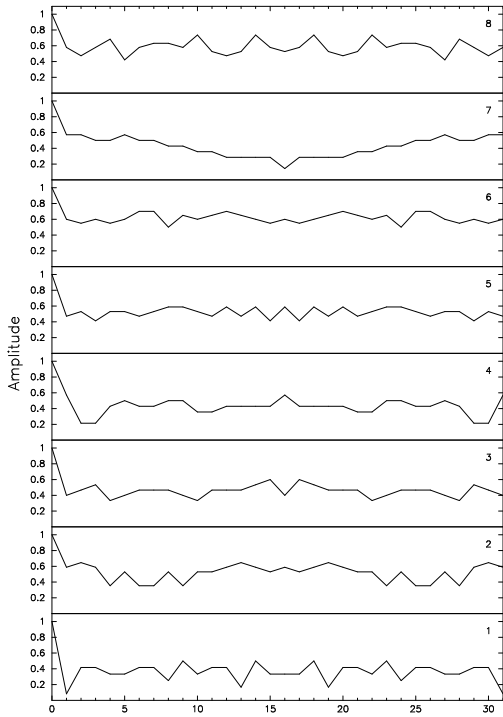


Shift (Elements)

Figure 12: 1-D Cyclic autocorrelation function row-wise for mask pattern 9-12

../CACFrow_Mask13.dat

../CACFrow_Mask14.dat

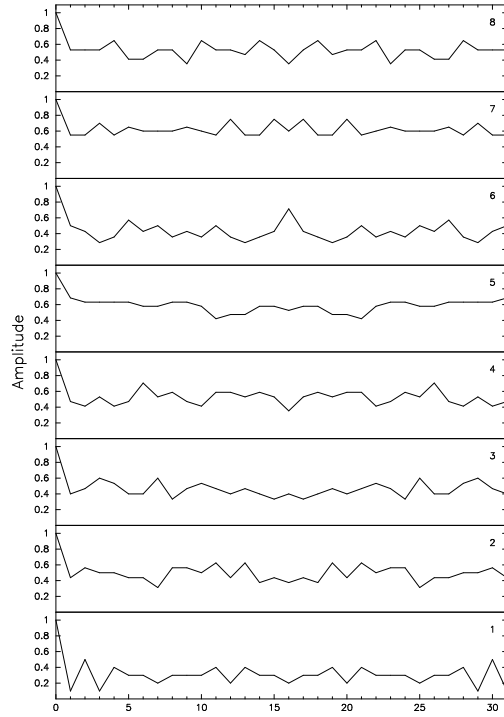
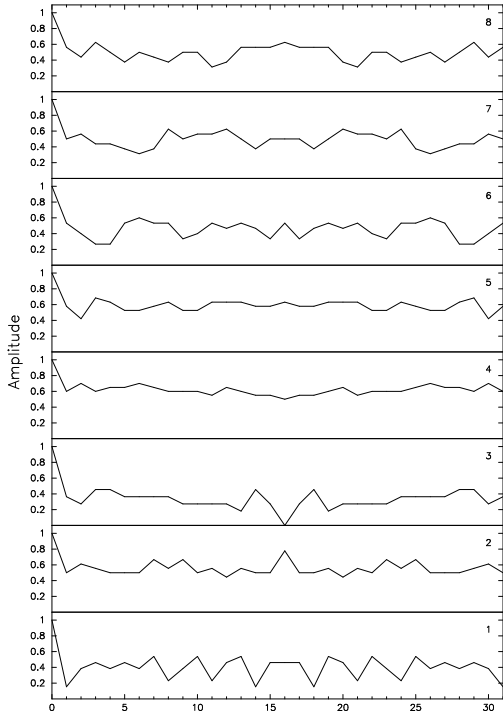


Shift (Elements)

Shift (Elements)

../CACFrow_Mask15.dat

../CACFrow_Mask16.dat



Shift (Elements)

Shift (Elements)

Figure 13: 1-D Cyclic autocorrelation function row-wise for mask pattern 13-16

FILE NAME	FOMrow1	FOMrow2	FOMrow3	FOMrow4	FOMrow5	FOMrow6	FOMrow7	FOMrow8	FOMtotal
LWrap1_m8.dat	6.930989	6.821045	4.953571	4.930149	7.971892	5.842374	5.503858	7.465112	50.418990
LWrap2_m8.dat	5.205165	5.509595	7.487057	5.869392	6.359988	7.275781	7.149270	6.950525	51.806775
LWrap3_m8.dat	9.688137	6.359988	6.044079	4.895281	5.590583	9.028424	5.983594	5.279876	52.869962
LWrap4_m8.dat	8.155534	7.465112	5.266057	7.695537	7.502091	5.056637	7.296333	5.345077	53.782378
LWrap5_m8.dat	3.345431	5.509595	6.767760	7.116355	4.325583	10.393022	8.242496	6.426592	52.126833
LWrap6_m8.dat	6.339588	5.663151	5.777086	7.392605	4.843324	5.662387	6.307890	7.106628	49.092658
LWrap7_m8.dat	5.205165	5.577852	5.842374	9.817152	7.465112	5.763505	10.253735	8.682704	58.607600
LWrap8_m8.dat	6.950525	6.095514	7.821713	5.680518	6.650916	9.398056	8.066324	7.922464	58.586028
LWrap9_m8.dat	5.141786	6.192883	5.941490	8.746426	5.941489	5.877621	8.242496	4.503585	50.587778
LWrap10_m8.dat	4.554036	3.627344	4.418939	9.352917	5.680519	9.764801	4.694285	6.339588	48.432429
LWrap11_m8.dat	3.327723	5.123644	7.294651	4.959899	6.076259	6.277730	8.810680	6.076259	47.946845
LWrap12_m8.dat	5.419402	7.922464	9.764802	5.877622	5.503859	6.640955	5.421101	8.066324	54.616529
LWrap13_m8.dat	5.869392	4.688577	7.922464	5.969620	8.170725	6.656404	4.953571	4.757043	48.987795
LWrap14_m8.dat	6.950525	5.662473	6.386986	4.651279	7.615844	7.190658	6.147739	4.812703	49.418208
LWrap15_m8.dat	4.812703	6.076259	6.945994	7.627702	6.615545	5.273730	5.662387	5.750269	48.764589
LWrap16_m8.dat	6.706818	5.939052	6.795772	5.751066	5.983595	6.076259	5.663151	5.577852	48.493566

Table 5: Figure of Merit: Row-wise

FILE NAME	FOMcol1	FOMcol2	FOMcol3	FOMcol4	FOMcol5	FOMcol6	FOMcol7	FOMcol8	FOMtotal
LWrap1_m8.dat	5.496915	6.188826	4.418939	6.640955	5.939052	6.152173	5.681540	3.832284	44.350684
LWrap2_m8.dat	5.208246	7.149271	6.138755	7.116355	5.139207	4.848346	4.140617	6.656403	46.397199
LWrap3_m8.dat	8.066324	4.953571	5.341867	3.851278	7.392605	5.680519	6.650916	6.650916	48.587995
LWrap4_m8.dat	5.939052	6.147739	4.955428	7.598085	8.242500	4.992191	6.586572	8.335419	52.796986
LWrap5_m8.dat	5.142678	7.190660	7.202940	4.646106	5.843953	5.154442	6.266282	5.969620	47.416680
LWrap6_m8.dat	5.509595	7.670035	5.498071	3.180055	5.843952	5.477226	5.941489	6.473158	45.593583
LWrap7_m8.dat	9.028424	7.892818	6.506606	6.192883	6.514945	6.795772	5.969620	6.568204	55.469272
LWrap8_m8.dat	5.503858	6.506606	6.152173	5.193386	6.998543	6.099944	4.640200	4.959899	46.054609
LWrap9_m8.dat	5.419402	6.821046	8.170726	3.701882	6.514945	5.082283	6.759126	7.627701	50.097110
LWrap10_m8.dat	7.116355	6.008620	5.419401	5.018643	4.459326	5.013072	6.260685	5.276388	44.572491
LWrap11_m8.dat	5.680519	5.341868	8.170726	6.863657	5.983594	5.498071	5.139207	4.953571	47.631213
LWrap12_m8.dat	6.076260	5.141786	6.650916	6.266282	4.449215	8.580426	4.002933	6.514945	47.682763
LWrap13_m8.dat	4.552270	5.079525	6.213960	5.842374	4.640200	4.839001	4.992191	4.646106	40.805626
LWrap14_m8.dat	7.726299	5.939052	3.824331	5.662473	5.353227	4.211716	4.449214	4.600976	41.767288
LWrap15_m8.dat	4.688577	9.083997	5.843952	8.242497	5.772170	5.139207	7.392604	6.950525	53.113528
LWrap16_m8.dat	6.506606	5.661535	3.305504	7.296335	7.695538	5.970603	5.276388	5.662473	47.374982

Table 6: Figure of Merit: Column-wise

A visual inspection shows pattern 8 to have minimum height of local peaks in the autocorrelation function. Pattern 8 does not correspond to the highest figure of merit for the low energy collimator, but is a close second to pattern 7 in this regard. Since pattern 7 is seen to have pronounced peaks in the 2-d autocorrelation function, we finally select pattern 8 as the optimum pattern of choice for fabrication.

Some attempts were made to quantify plots 14 to 29. Plots 30 to 33 display the linear plot of linear autocorrelation versus $\sqrt{k^2 + m^2}$ and to all these plots fitting was performed and its reduced chisquare (figure of merit) values were noted. The scatter in these linear plots are more pronounced and hence drowns the peaks visible in the 2-d plots. Hence we select pattern 8 as the optimum pattern for the CAM.

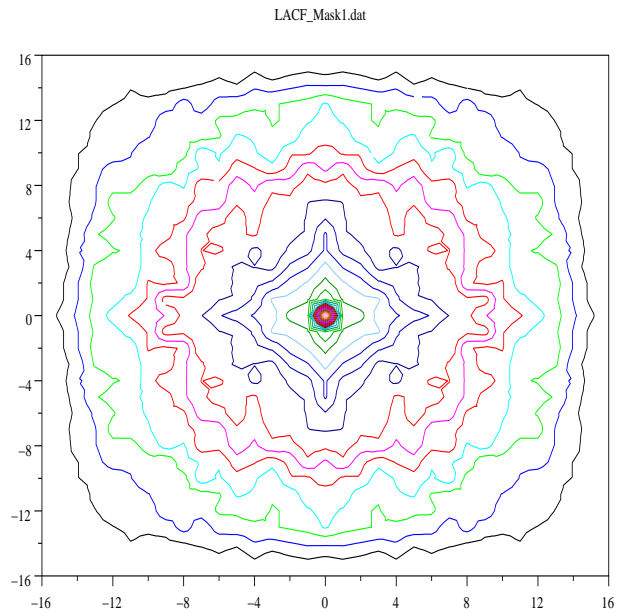
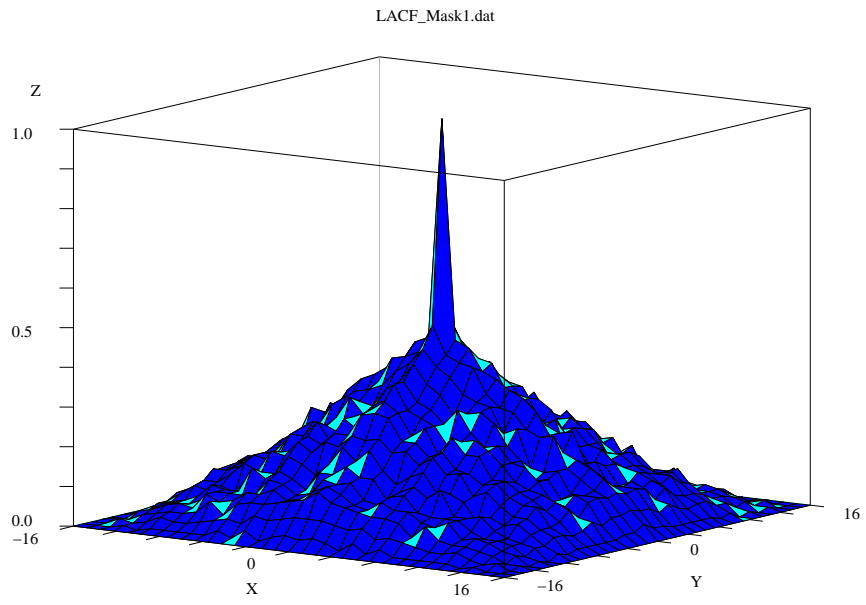


Figure 14: 2-D Linear autocorrelation function

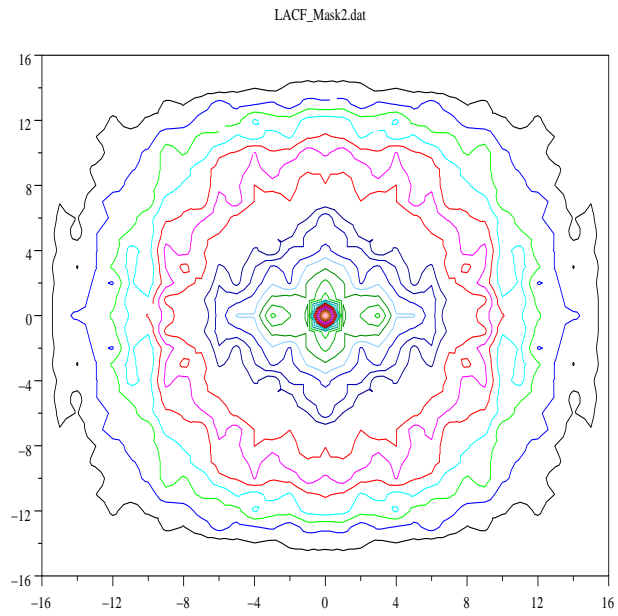
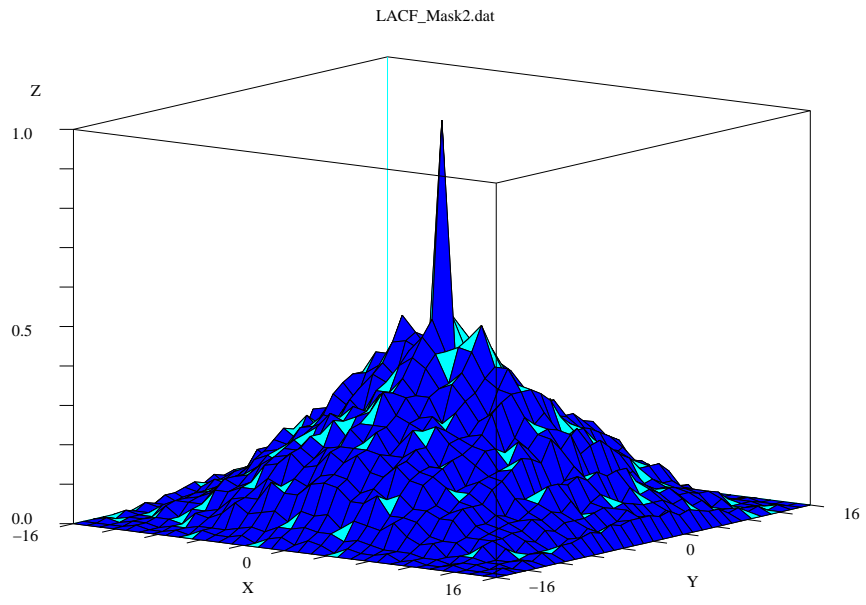


Figure 15: 2-D Linear autocorrelation function

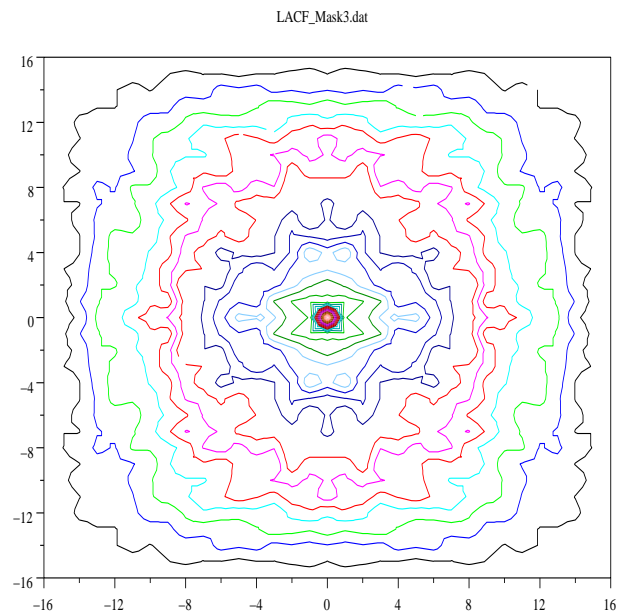
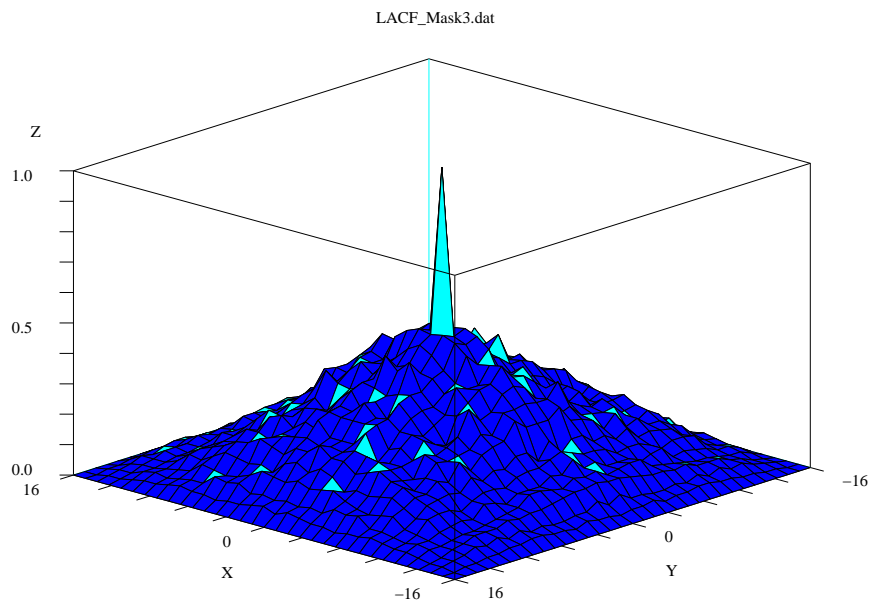


Figure 16: 2-D Linear autocorrelation function

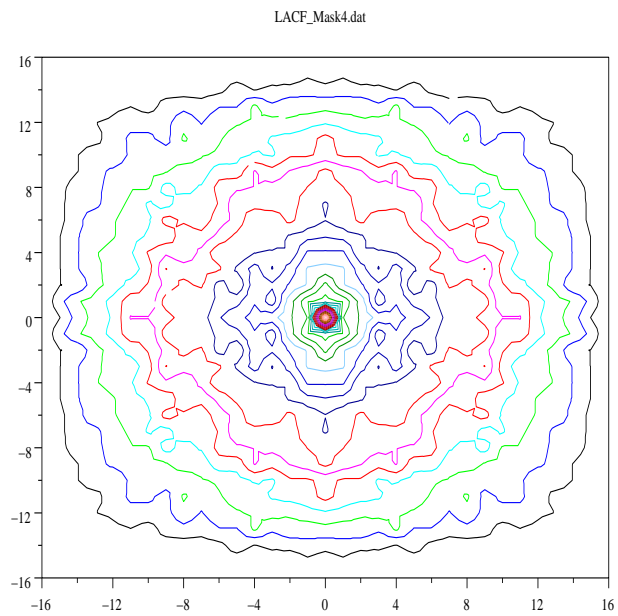
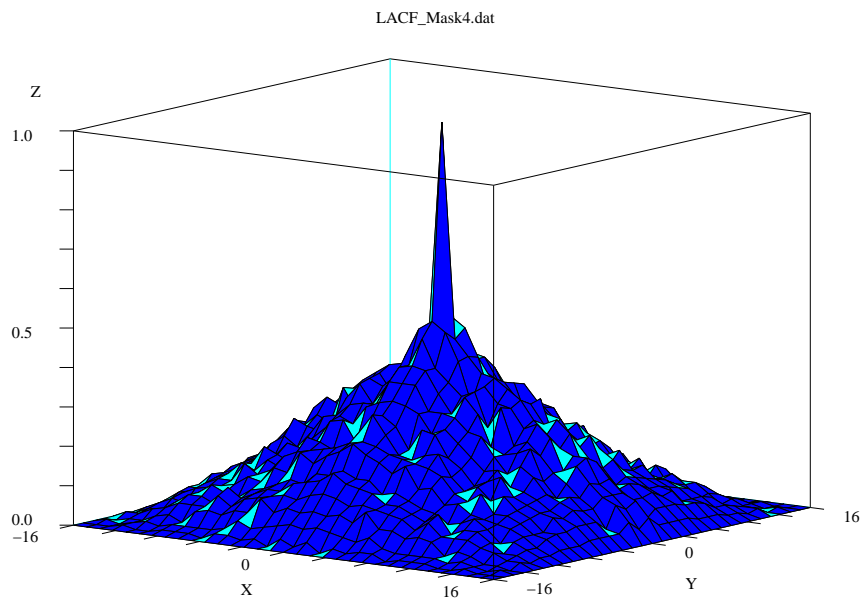


Figure 17: 2-D Linear autocorrelation function

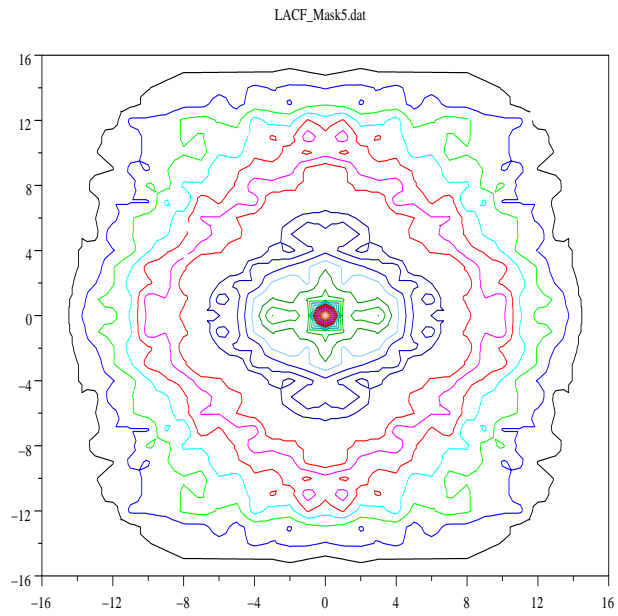
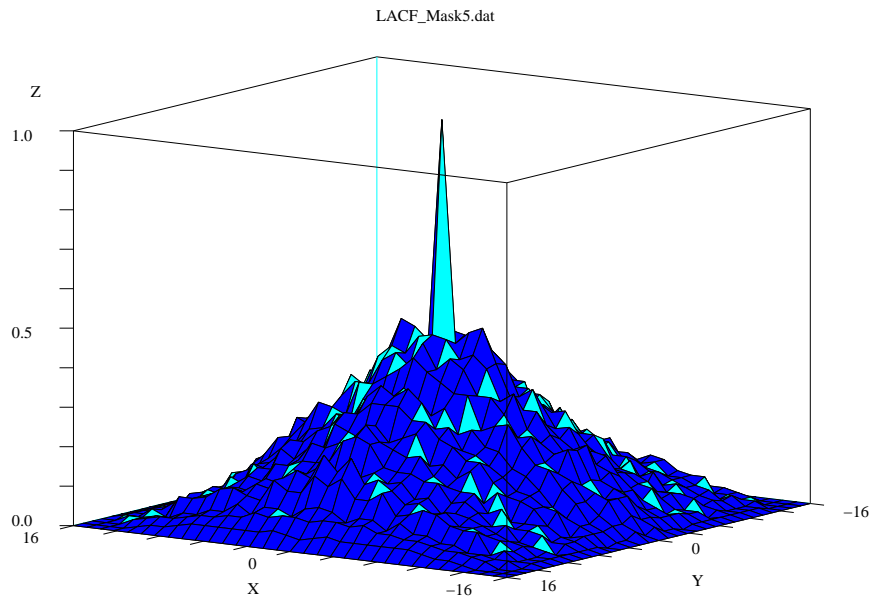


Figure 18: 2-D Linear autocorrelation function

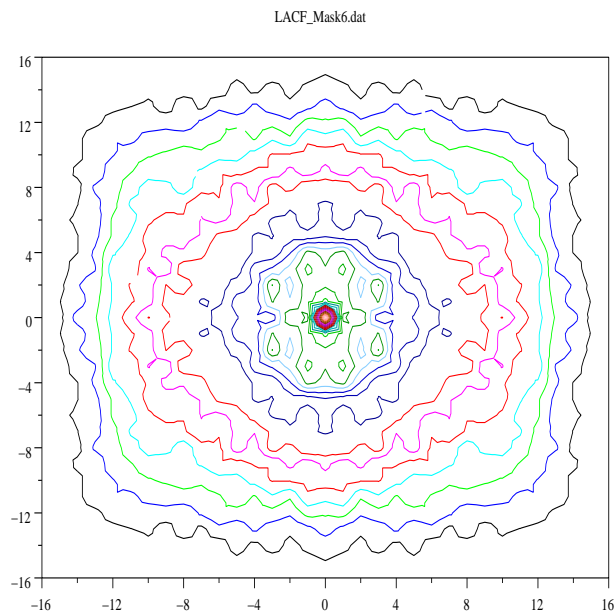
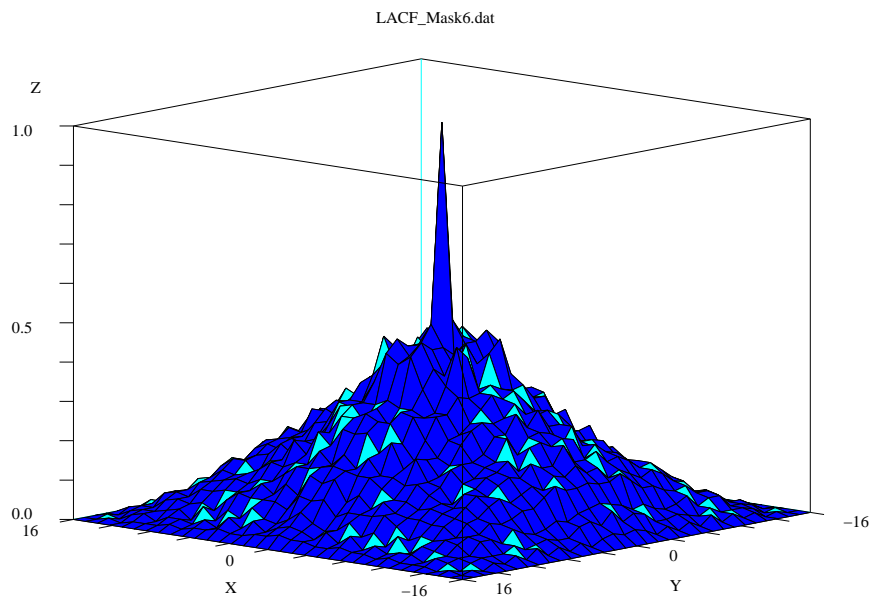


Figure 19: 2-D Linear autocorrelation function

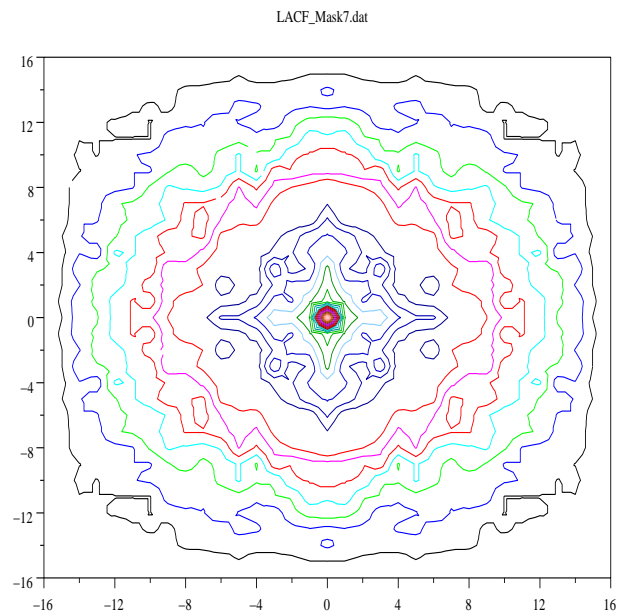
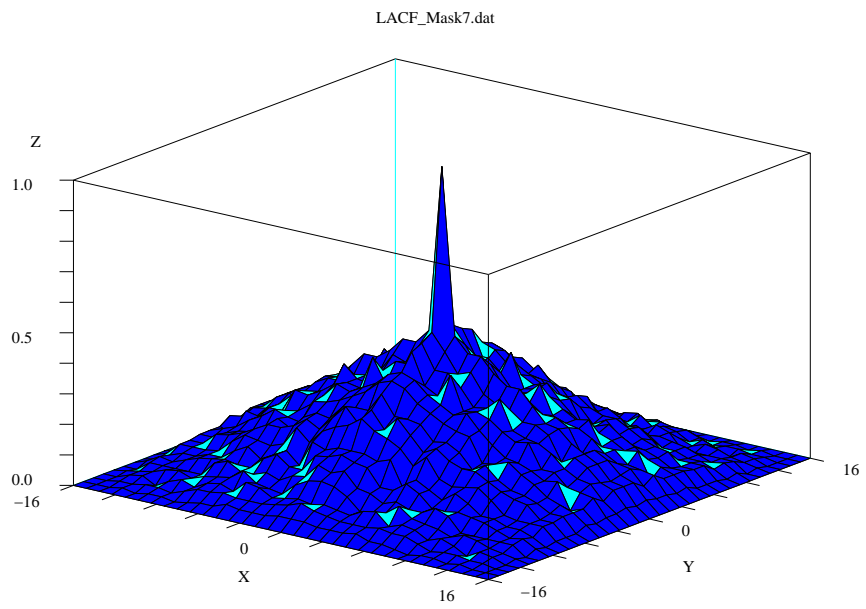


Figure 20: 2-D Linear autocorrelation function

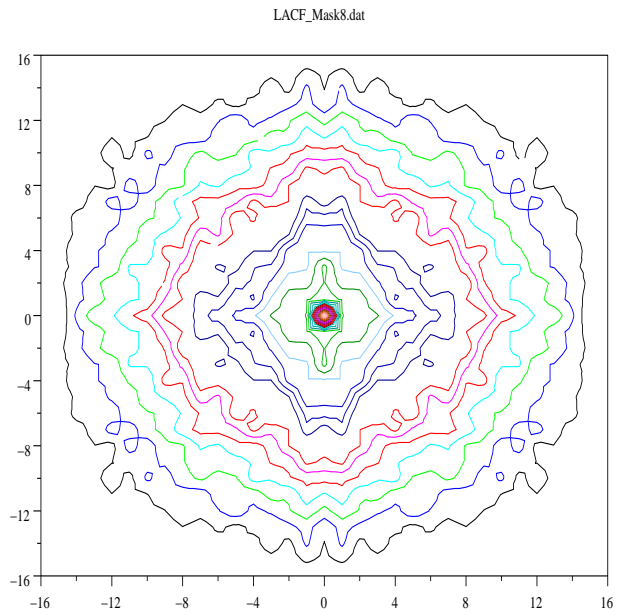
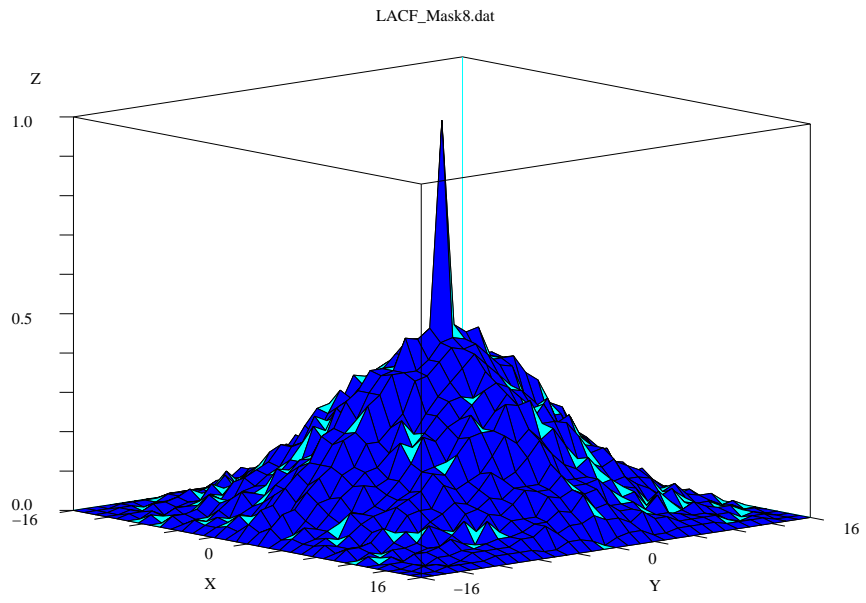


Figure 21: 2-D Linear autocorrelation function

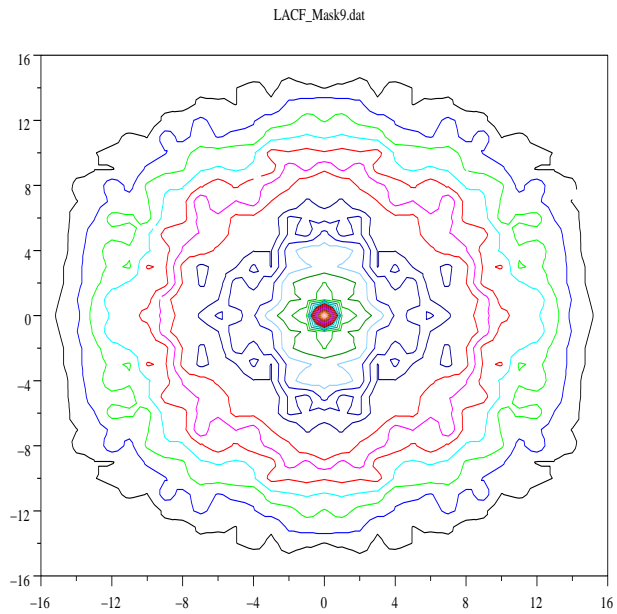
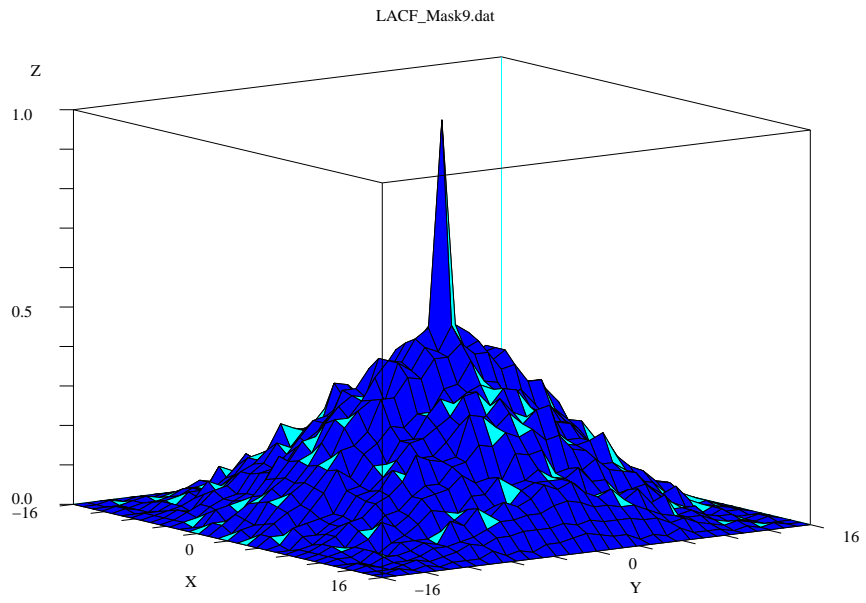


Figure 22: 2-D Linear autocorrelation function

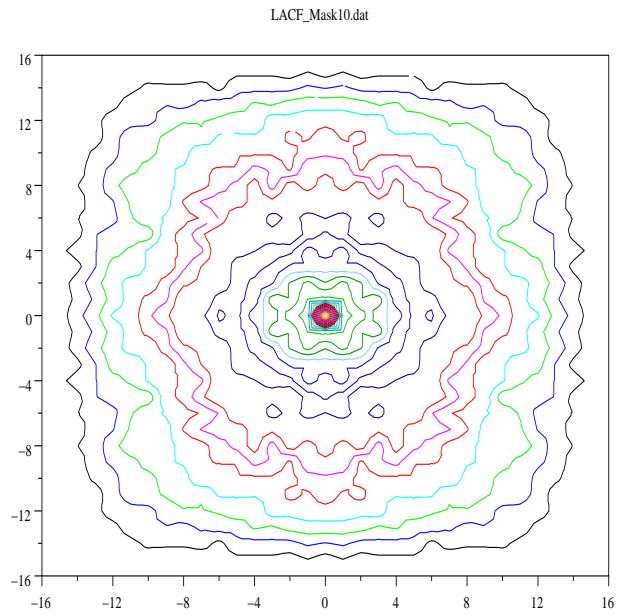
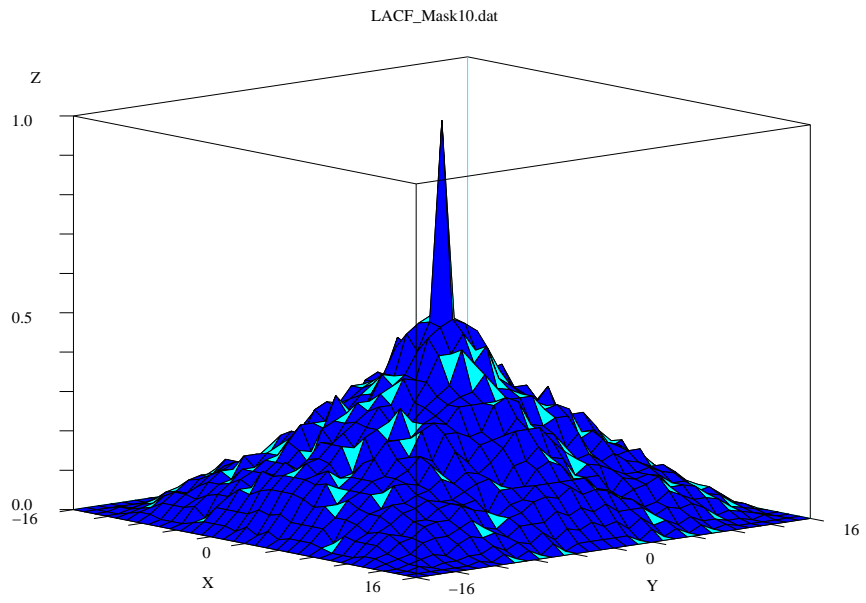


Figure 23: 2-D Linear autocorrelation function

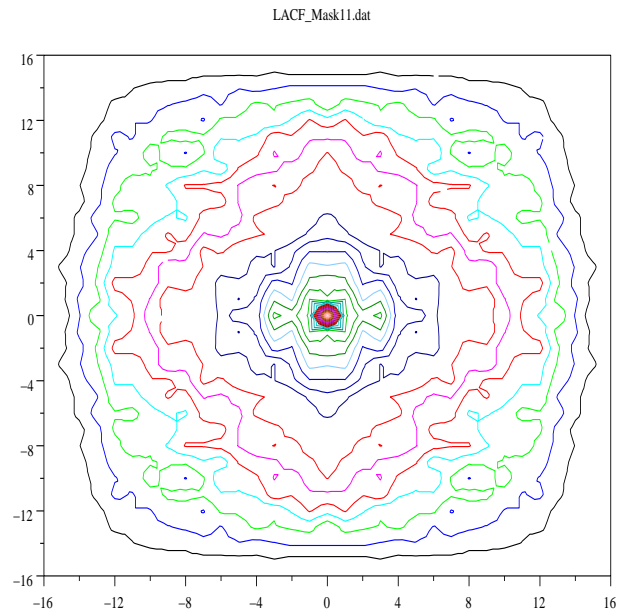
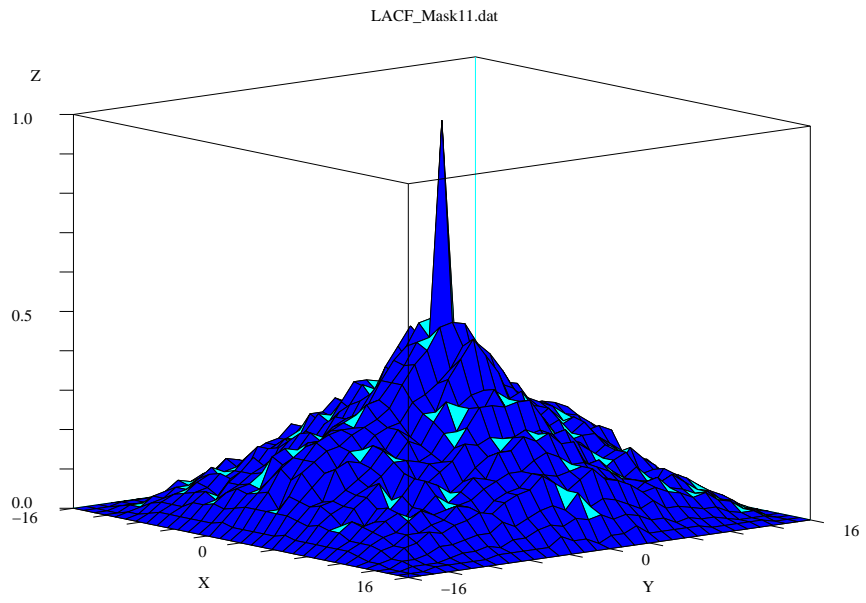


Figure 24: 2-D Linear autocorrelation function

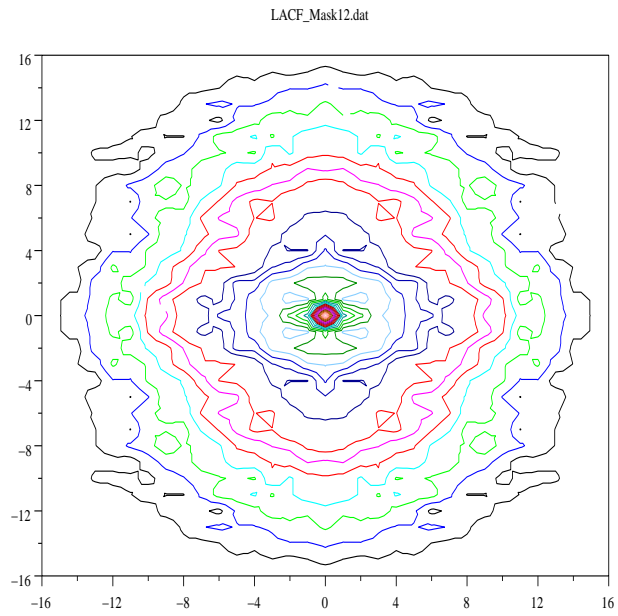
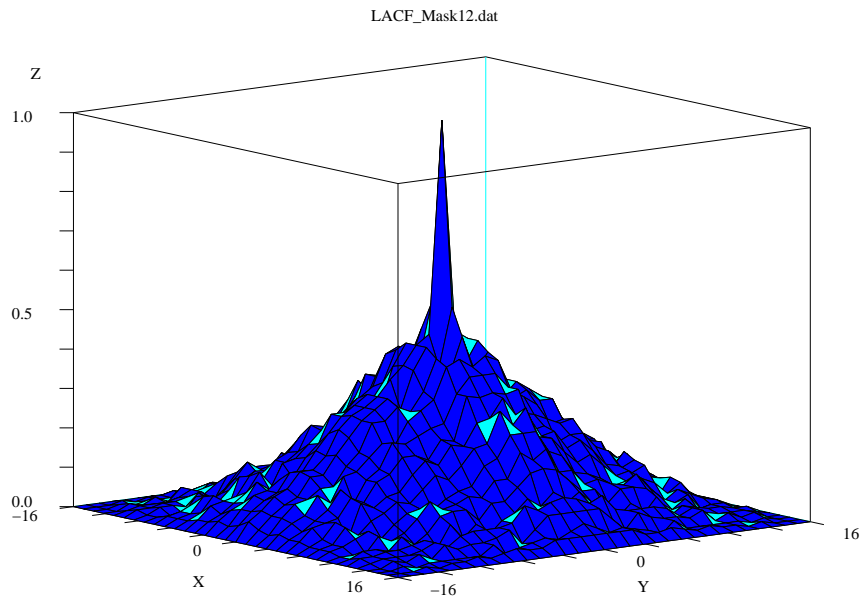


Figure 25: 2-D Linear autocorrelation function

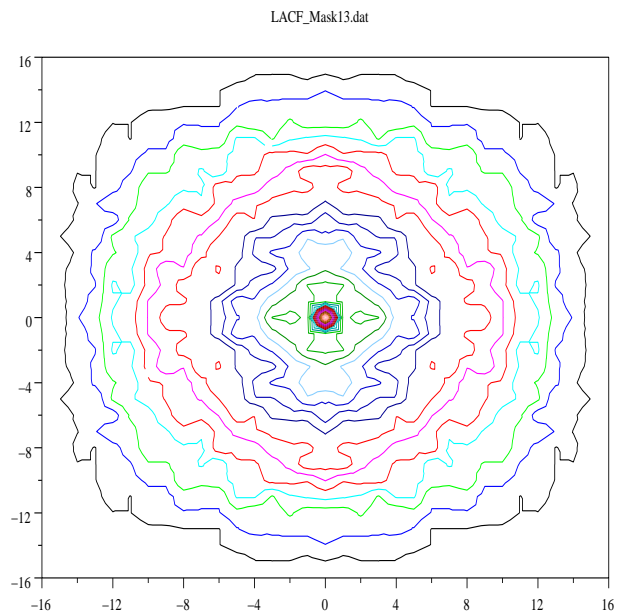
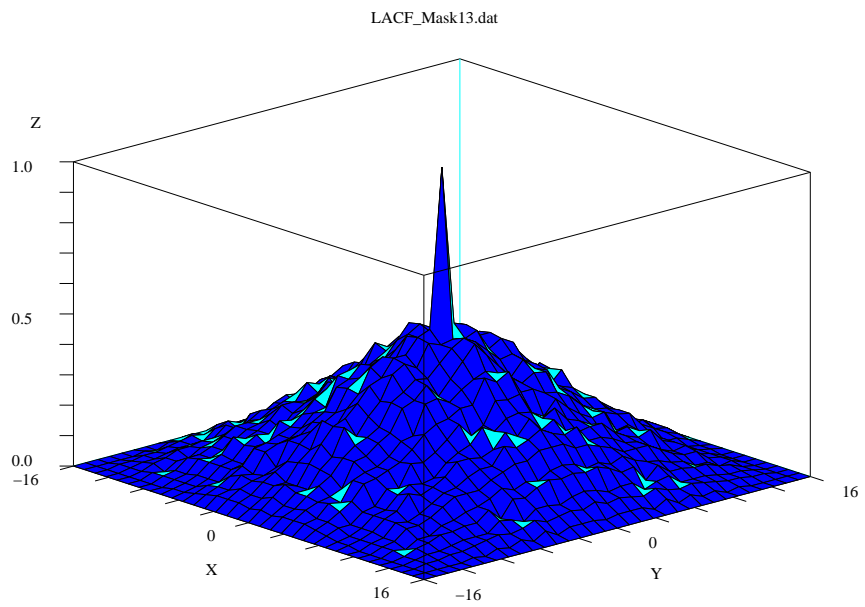


Figure 26: 2-D Linear autocorrelation function

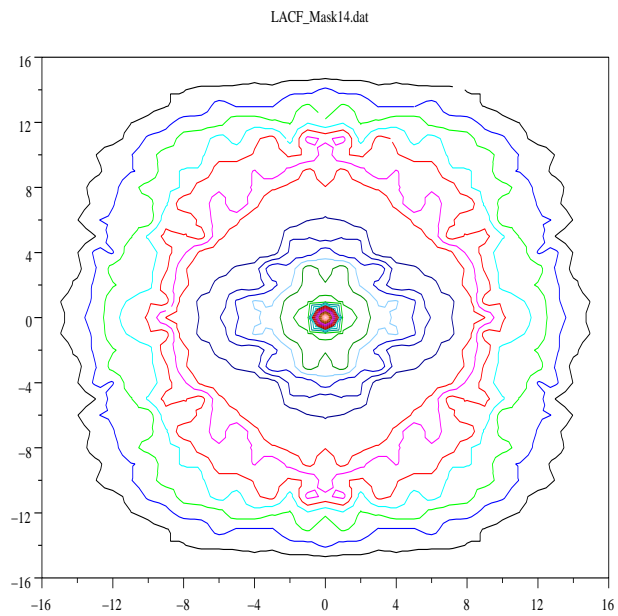
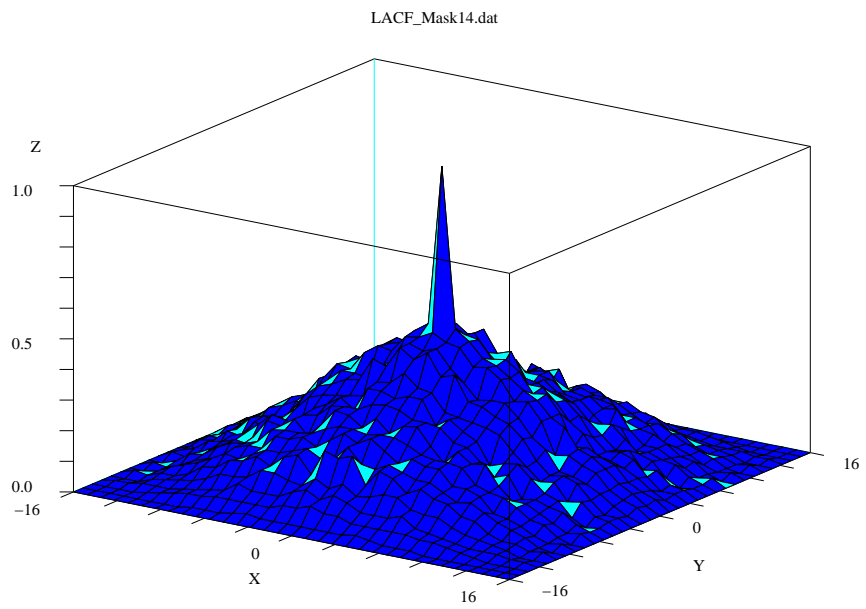


Figure 27: 2-D Linear autocorrelation function

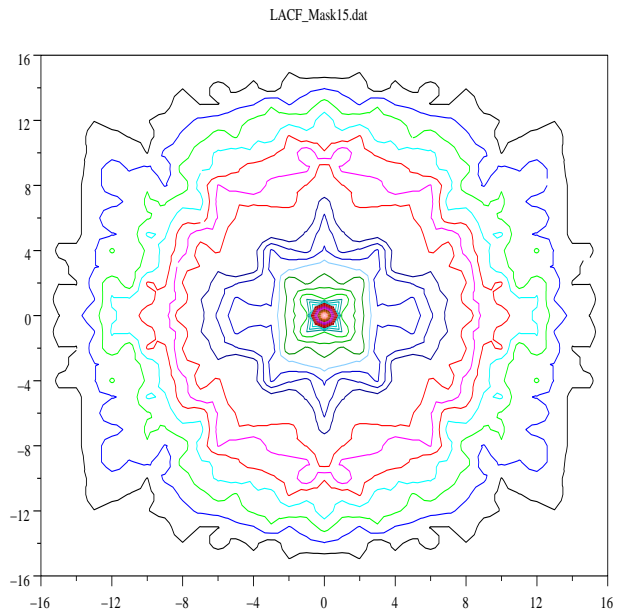
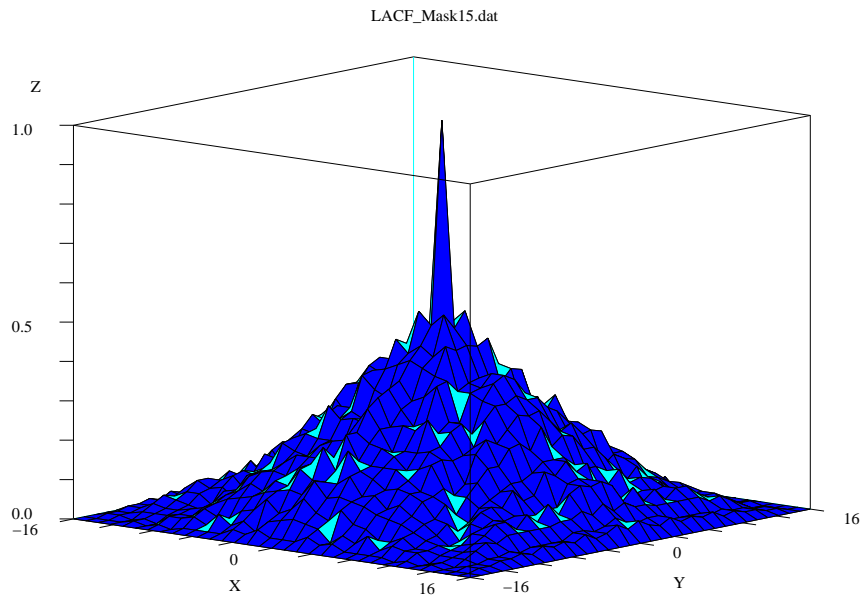


Figure 28: 2-D Linear autocorrelation function

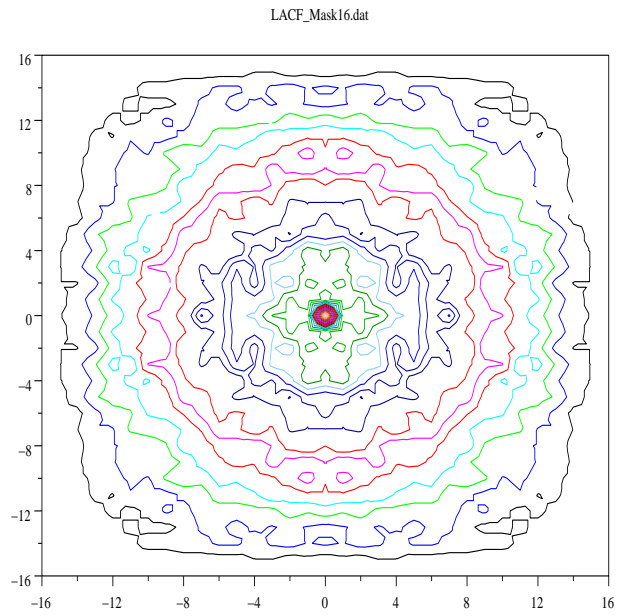
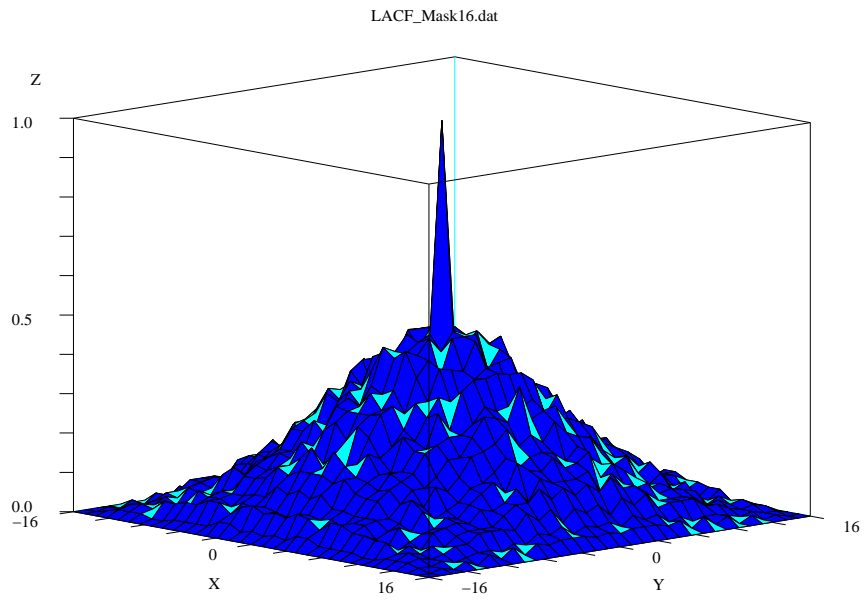


Figure 29: 2-D Linear autocorrelation function

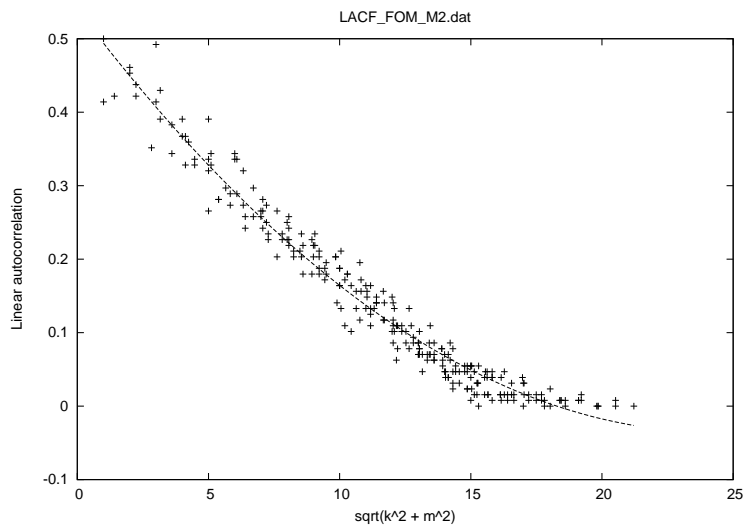
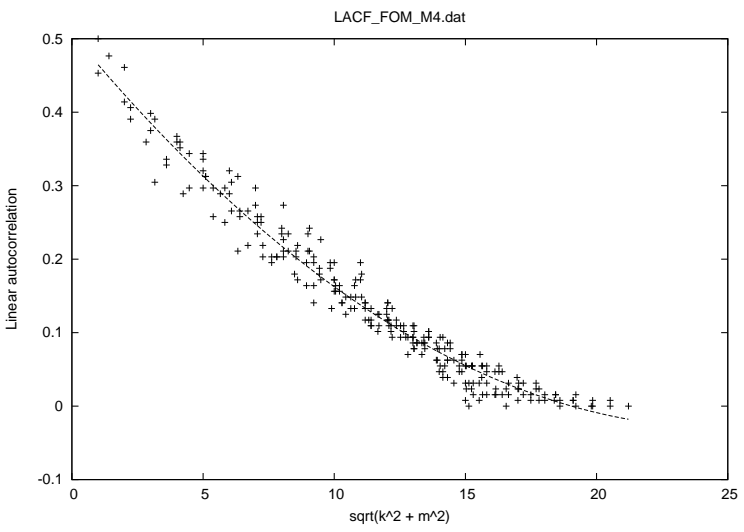
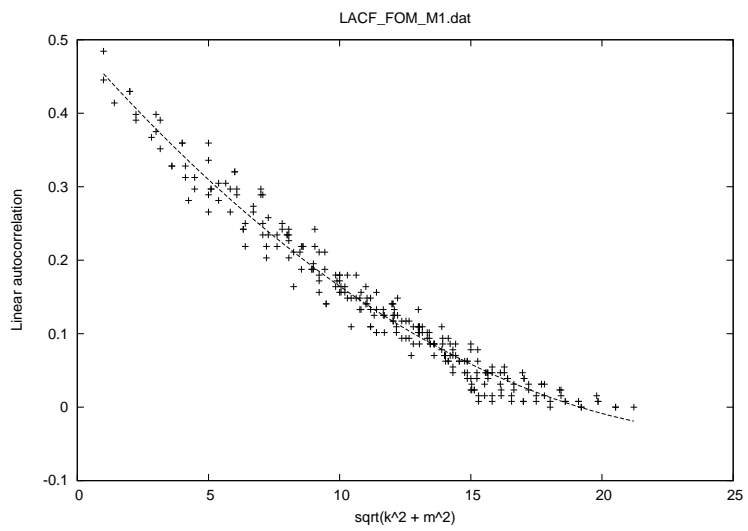
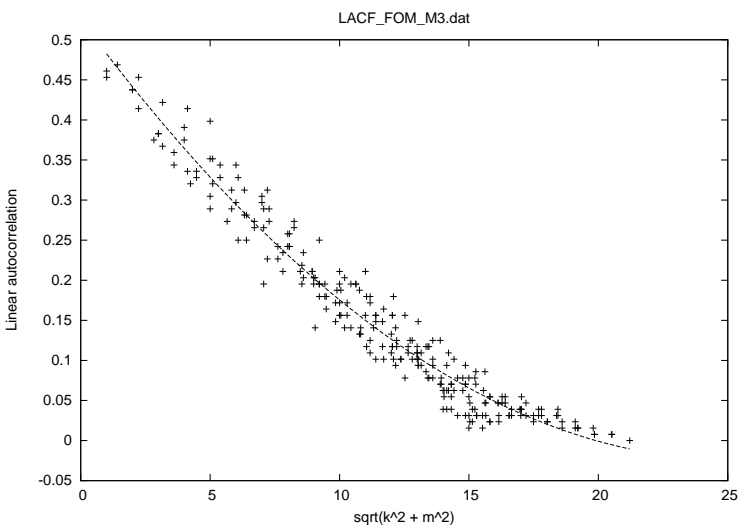


Figure 30: Plot of LACF $v/s \sqrt{k^2 + m^2}$ for mask pattern 1, 2, 3 and 4

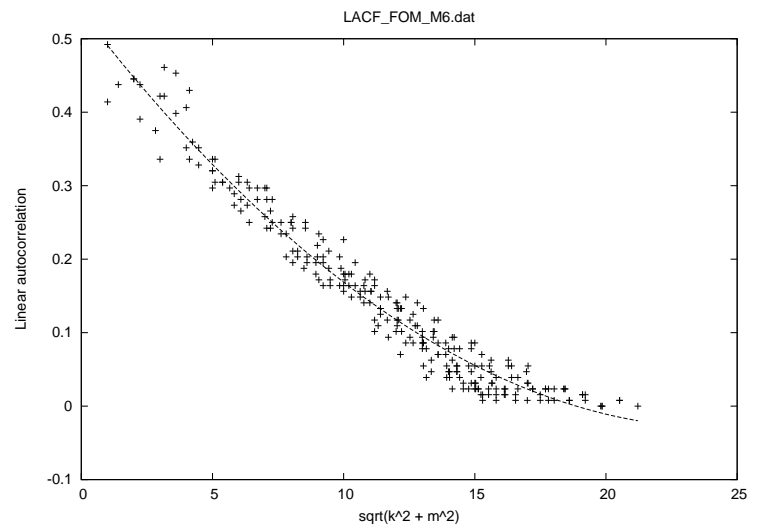
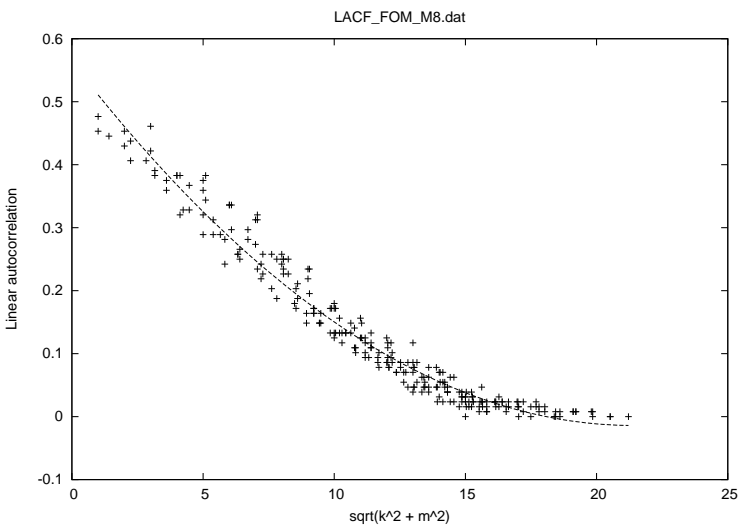
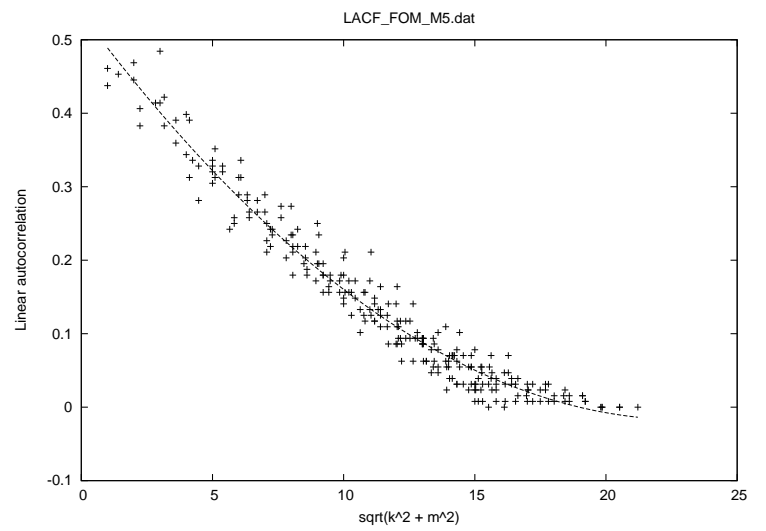
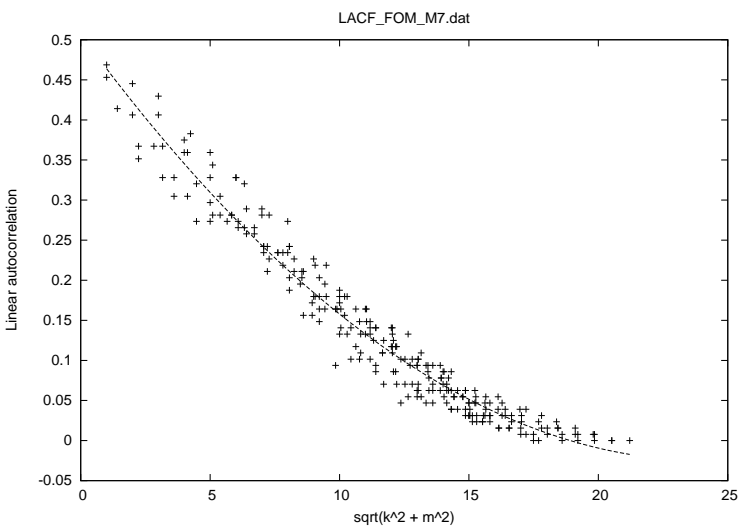


Figure 31: Plot of LACF v/s $\sqrt{k^2 + m^2}$ for mask pattern 5, 6, 7 and 8

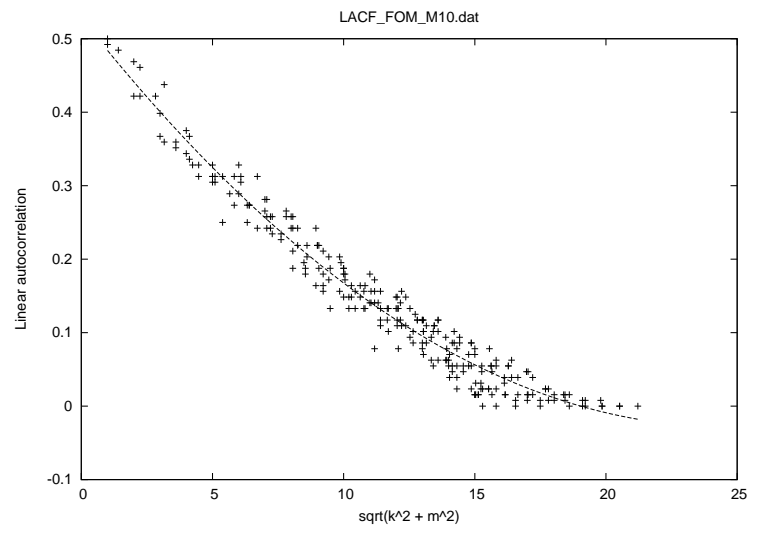
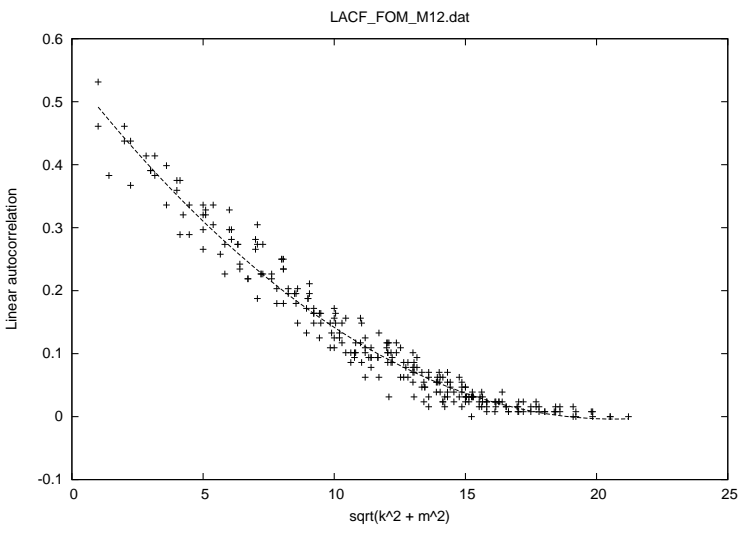
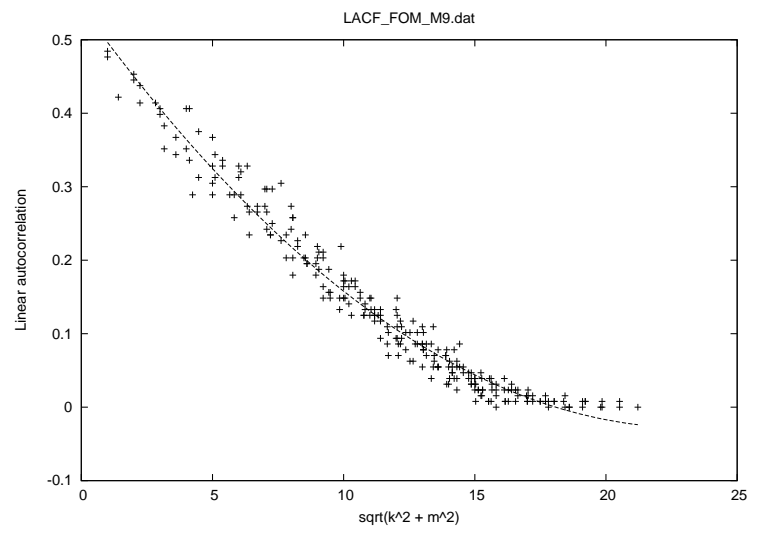
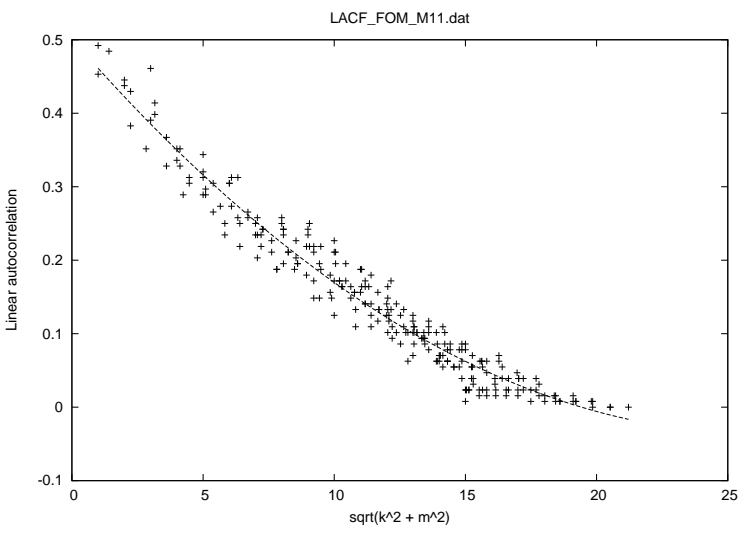


Figure 32: Plot of LACF v/s $\sqrt{k^2 + m^2}$ for mask pattern 9, 10, 11 and 12

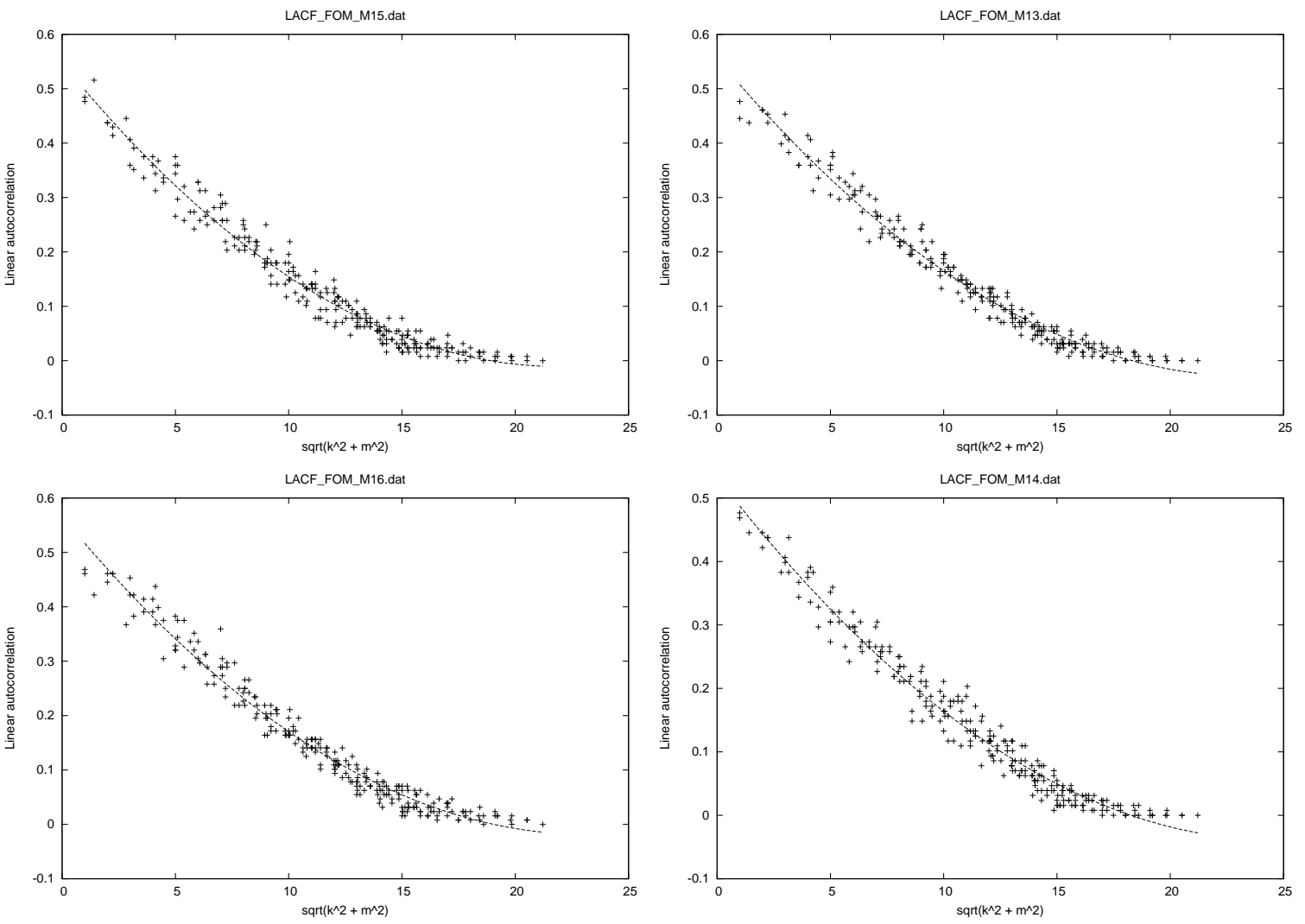


Figure 33: Plot of LACF v/s $\sqrt{k^2 + m^2}$ for mask pattern 13, 14, 15 and 16

Wed Nov 5 10:37:49 2003

FIT: data read from "LACF_FOM_M1.dat"
#datapoints = 255
residuals are weighted equally (unit weight)

function used for fitting: $f(x) = a + b*x + c*x**2$
fitted parameters initialized with current variable values

Iteration 0

WSSR : 1.00485e+07 delta(WSSR)/WSSR : 0
delta(WSSR) : 0 limit for stopping : 1e-05
lambda : 107.382

initial set of free parameter values

a = 1
b = 1
c = 1

After 5 iterations the fit converged.
final sum of squares of residuals : 0.0961523
rel. change during last iteration : -1.58505e-07

degrees of freedom (ndf) : 252
rms of residuals (stdfit) = $\sqrt{\text{WSSR}/\text{ndf}}$: 0.0195335
variance of residuals (reduced chisquare) = WSSR/ndf : 0.000381557

Final set of parameters	Asymptotic Standard Error
=====	=====
a = 0.49362	+/- 0.006289 (1.274%)
b = -0.0406717	+/- 0.001194 (2.935%)
c = 0.000778123	+/- 5.295e-05 (6.804%)

correlation matrix of the fit parameters:

	a	b	c
a	1.000		
b	-0.934	1.000	
c	0.841	-0.974	1.000

Wed Nov 5 10:44:34 2003

FIT: data read from "LACF_FOM_M2.dat"
#datapoints = 255
residuals are weighted equally (unit weight)

function used for fitting: $f(x) = a + b*x + c*x**2$
fitted parameters initialized with current variable values

Iteration 0

WSSR : 0.163477 delta(WSSR)/WSSR : 0
delta(WSSR) : 0 limit for stopping : 1e-05
lambda : 107.382

initial set of free parameter values

a = 0.49362
b = -0.0406717
c = 0.000778901

After 5 iterations the fit converged.
final sum of squares of residuals : 0.128534
rel. change during last iteration : -2.50831e-09

degrees of freedom (ndf) : 252
rms of residuals (stdfit) = $\sqrt{\text{WSSR}/\text{ndf}}$: 0.0225844
variance of residuals (reduced chisquare) = WSSR/ndf : 0.000510057

Final set of parameters		Asymptotic Standard Error	
=====		=====	
a	= 0.540169	+/- 0.007272	(1.346%)
b	= -0.0472908	+/- 0.00138	(2.919%)
c	= 0.000970586	+/- 6.122e-05	(6.307%)

correlation matrix of the fit parameters:

	a	b	c
a	1.000		
b	-0.934	1.000	
c	0.841	-0.974	1.000

Wed Nov 5 10:50:17 2003

FIT: data read from "LACF_FOM_M3.dat"
#datapoints = 255
residuals are weighted equally (unit weight)

function used for fitting: $f(x) = a + b*x + c*x**2$
fitted parameters initialized with current variable values

Iteration 0

WSSR : 0.186739 delta(WSSR)/WSSR : 0
delta(WSSR) : 0 limit for stopping : 1e-05
lambda : 107.382

initial set of free parameter values

a = 0.540169
b = -0.0472908
c = 0.000970586

After 5 iterations the fit converged.
final sum of squares of residuals : 0.142463
rel. change during last iteration : -2.42651e-10

degrees of freedom (ndf) : 252
rms of residuals (stdfit) = $\sqrt{\text{WSSR}/\text{ndf}}$: 0.0237766
variance of residuals (reduced chisquare) = WSSR/ndf : 0.000565328

Final set of parameters	Asymptotic Standard Error
=====	=====
a = 0.525192	+/- 0.007655 (1.458%)
b = -0.0436363	+/- 0.001453 (3.33%)
c = 0.0008667	+/- 6.445e-05 (7.436%)

correlation matrix of the fit parameters:

	a	b	c
a	1.000		
b	-0.934	1.000	
c	0.841	-0.974	1.000

Wed Nov 5 10:54:19 2003

FIT: data read from "LACF_FOM_M4.dat"
#datapoints = 255
residuals are weighted equally (unit weight)

function used for fitting: $f(x) = a + b*x + c*x**2$
fitted parameters initialized with current variable values

Iteration 0

WSSR : 0.148097 delta(WSSR)/WSSR : 0
delta(WSSR) : 0 limit for stopping : 1e-05
lambda : 107.382

initial set of free parameter values

a = 0.525192
b = -0.0436363
c = 0.0008667

After 5 iterations the fit converged.
final sum of squares of residuals : 0.109406
rel. change during last iteration : -4.41909e-10

degrees of freedom (ndf) : 252
rms of residuals (stdfit) = $\sqrt{WSSR/ndf}$: 0.0208363
variance of residuals (reduced chisquare) = $WSSR/ndf$: 0.000434152

Final set of parameters	Asymptotic Standard Error
=====	=====
a = 0.506813	+/- 0.006709 (1.324%)
b = -0.0430544	+/- 0.001273 (2.958%)
c = 0.000863512	+/- 5.648e-05 (6.541%)

correlation matrix of the fit parameters:

	a	b	c
a	1.000		
b	-0.934	1.000	
c	0.841	-0.974	1.000

Wed Nov 5 10:58:34 2003

FIT: data read from "LACF_FOM_M5.dat"
#datapoints = 255
residuals are weighted equally (unit weight)

function used for fitting: $f(x) = a + b*x + c*x**2$
fitted parameters initialized with current variable values

Iteration 0

WSSR : 0.144815 delta(WSSR)/WSSR : 0
delta(WSSR) : 0 limit for stopping : 1e-05
lambda : 107.382

initial set of free parameter values

a = 0.506813
b = -0.0430544
c = 0.000863512

After 5 iterations the fit converged.
final sum of squares of residuals : 0.134967
rel. change during last iteration : -9.35905e-10

degrees of freedom (ndf) : 252
rms of residuals (stdfit) = $\sqrt{\text{WSSR}/\text{ndf}}$: 0.0231427
variance of residuals (reduced chisquare) = WSSR/ndf : 0.000535585

Final set of parameters	Asymptotic Standard Error
=====	=====
a = 0.535815	+/- 0.007451 (1.391%)
b = -0.0479486	+/- 0.001414 (2.95%)
c = 0.00103911	+/- 6.273e-05 (6.037%)

correlation matrix of the fit parameters:

	a	b	c
a	1.000		
b	-0.934	1.000	
c	0.841	-0.974	1.000

Wed Nov 5 11:00:40 2003

FIT: data read from "LACF_FOM_M6.dat"
#datapoints = 255
residuals are weighted equally (unit weight)

function used for fitting: $f(x) = a + b*x + c*x**2$
fitted parameters initialized with current variable values

Iteration 0

WSSR : 0.151013 delta(WSSR)/WSSR : 0
delta(WSSR) : 0 limit for stopping : 1e-05
lambda : 107.382

initial set of free parameter values

a = 0.535815
b = -0.0479486
c = 0.00103911

After 4 iterations the fit converged.
final sum of squares of residuals : 0.139987
rel. change during last iteration : -2.32478e-08

degrees of freedom (ndf) : 252
rms of residuals (stdfit) = $\sqrt{WSSR/ndf}$: 0.0235691
variance of residuals (reduced chisquare) = $WSSR/ndf$: 0.000555502

Final set of parameters	Asymptotic Standard Error
=====	=====
a = 0.535959	+/- 0.007589 (1.416%)
b = -0.0460992	+/- 0.00144 (3.125%)
c = 0.000937836	+/- 6.389e-05 (6.812%)

correlation matrix of the fit parameters:

	a	b	c
a	1.000		
b	-0.934	1.000	
c	0.841	-0.974	1.000

Wed Nov 5 11:02:47 2003

FIT: data read from "LACF_FOM_M7.dat"
#datapoints = 255
residuals are weighted equally (unit weight)

function used for fitting: $f(x) = a + b*x + c*x**2$
fitted parameters initialized with current variable values

Iteration 0

WSSR : 0.159557 delta(WSSR)/WSSR : 0
delta(WSSR) : 0 limit for stopping : 1e-05
lambda : 107.382

initial set of free parameter values

a = 0.535959
b = -0.0460992
c = 0.000937836

After 5 iterations the fit converged.
final sum of squares of residuals : 0.127203
rel. change during last iteration : -9.61072e-10

degrees of freedom (ndf) : 252
rms of residuals (stdfit) = $\sqrt{\text{WSSR}/\text{ndf}}$: 0.0224672
variance of residuals (reduced chisquare) = WSSR/ndf : 0.000504775

Final set of parameters	Asymptotic Standard Error
=====	=====
a = 0.506939	+/- 0.007234 (1.427%)
b = -0.0440175	+/- 0.001373 (3.119%)
c = 0.000910137	+/- 6.09e-05 (6.691%)

correlation matrix of the fit parameters:

	a	b	c
a	1.000		
b	-0.934	1.000	
c	0.841	-0.974	1.000

Wed Nov 5 11:05:15 2003

FIT: data read from "LACF_FOM_M8.dat"
#datapoints = 255
residuals are weighted equally (unit weight)

function used for fitting: $f(x) = a + b*x + c*x**2$
fitted parameters initialized with current variable values

Iteration 0

WSSR : 0.172314 delta(WSSR)/WSSR : 0
delta(WSSR) : 0 limit for stopping : 1e-05
lambda : 107.382

initial set of free parameter values

a = 0.506939
b = -0.0440175
c = 0.000910137

After 5 iterations the fit converged.
final sum of squares of residuals : 0.125013
rel. change during last iteration : -3.8384e-09

degrees of freedom (ndf) : 252
rms of residuals (stdfit) = $\sqrt{\text{WSSR}/\text{ndf}}$: 0.0222729
variance of residuals (reduced chisquare) = WSSR/ndf : 0.000496082

Final set of parameters	Asymptotic Standard Error
=====	=====
a = 0.56341	+/- 0.007171 (1.273%)
b = -0.0538757	+/- 0.001361 (2.527%)
c = 0.00125653	+/- 6.037e-05 (4.805%)

correlation matrix of the fit parameters:

	a	b	c
a	1.000		
b	-0.934	1.000	
c	0.841	-0.974	1.000

Wed Nov 5 11:08:18 2003

FIT: data read from "LACF_FOM_M9.dat"
#datapoints = 255
residuals are weighted equally (unit weight)

function used for fitting: $f(x) = a + b*x + c*x**2$
fitted parameters initialized with current variable values

Iteration 0

WSSR : 0.123514 delta(WSSR)/WSSR : 0
delta(WSSR) : 0 limit for stopping : 1e-05
lambda : 107.382

initial set of free parameter values

a = 0.56341
b = -0.0538757
c = 0.00125653

After 5 iterations the fit converged.
final sum of squares of residuals : 0.113404
rel. change during last iteration : -4.76826e-10

degrees of freedom (ndf) : 252
rms of residuals (stdfit) = $\sqrt{\text{WSSR}/\text{ndf}}$: 0.0212136
variance of residuals (reduced chisquare) = WSSR/ndf : 0.000450015

Final set of parameters	Asymptotic Standard Error
=====	=====
a = 0.544684	+/- 0.00683 (1.254%)
b = -0.0492709	+/- 0.001296 (2.631%)
c = 0.00105918	+/- 5.75e-05 (5.429%)

correlation matrix of the fit parameters:

	a	b	c
a	1.000		
b	-0.934	1.000	
c	0.841	-0.974	1.000

Wed Nov 5 11:11:17 2003

FIT: data read from "LACF_FOM_M10.dat"
#datapoints = 255
residuals are weighted equally (unit weight)

function used for fitting: $f(x) = a + b*x + c*x**2$
fitted parameters initialized with current variable values

Iteration 0

WSSR : 0.144686 delta(WSSR)/WSSR : 0
delta(WSSR) : 0 limit for stopping : 1e-05
lambda : 107.382

initial set of free parameter values

a = 0.544684
b = -0.0492709
c = 0.00105918

After 5 iterations the fit converged.
final sum of squares of residuals : 0.118792
rel. change during last iteration : -3.47682e-10

degrees of freedom (ndf) : 252
rms of residuals (stdfit) = $\sqrt{\text{WSSR}/\text{ndf}}$: 0.0217117
variance of residuals (reduced chisquare) = WSSR/ndf : 0.000471398

Final set of parameters	Asymptotic Standard Error
=====	=====
a = 0.528313	+/- 0.006991 (1.323%)
b = -0.0452792	+/- 0.001327 (2.93%)
c = 0.000920712	+/- 5.885e-05 (6.392%)

correlation matrix of the fit parameters:

	a	b	c
a	1.000		
b	-0.934	1.000	
c	0.841	-0.974	1.000

Wed Nov 5 11:14:06 2003

FIT: data read from "LACF_FOM_M11.dat"
#datapoints = 255
residuals are weighted equally (unit weight)

function used for fitting: $f(x) = a + b*x + c*x**2$
fitted parameters initialized with current variable values

Iteration 0

WSSR : 0.143035 delta(WSSR)/WSSR : 0
delta(WSSR) : 0 limit for stopping : 1e-05
lambda : 107.382

initial set of free parameter values

a = 0.528313
b = -0.0452792
c = 0.000920712

After 5 iterations the fit converged.
final sum of squares of residuals : 0.132052
rel. change during last iteration : -8.28337e-10

degrees of freedom (ndf) : 252
rms of residuals (stdfit) = $\sqrt{\text{WSSR}/\text{ndf}}$: 0.0228914
variance of residuals (reduced chisquare) = WSSR/ndf : 0.000524018

Final set of parameters	Asymptotic Standard Error
=====	=====
a = 0.501282	+/- 0.00737 (1.47%)
b = -0.0409588	+/- 0.001399 (3.416%)
c = 0.000780096	+/- 6.205e-05 (7.954%)

correlation matrix of the fit parameters:

	a	b	c
a	1.000		
b	-0.934	1.000	
c	0.841	-0.974	1.000

Wed Nov 5 11:16:18 2003

FIT: data read from "LACF_FOM_M12.dat"
#datapoints = 255
residuals are weighted equally (unit weight)

function used for fitting: $f(x) = a + b*x + c*x**2$
fitted parameters initialized with current variable values

Iteration 0

WSSR : 0.264372 delta(WSSR)/WSSR : 0
delta(WSSR) : 0 limit for stopping : 1e-05
lambda : 107.382

initial set of free parameter values

a = 0.501282
b = -0.0409588
c = 0.000780096

After 5 iterations the fit converged.
final sum of squares of residuals : 0.125443
rel. change during last iteration : -2.19111e-09

degrees of freedom (ndf) : 252
rms of residuals (stdfit) = $\sqrt{\text{WSSR}/\text{ndf}}$: 0.0223112
variance of residuals (reduced chisquare) = WSSR/ndf : 0.000497788

Final set of parameters	Asymptotic Standard Error
=====	=====
a = 0.543209	+/- 0.007184 (1.322%)
b = -0.0529725	+/- 0.001364 (2.574%)
c = 0.00128236	+/- 6.048e-05 (4.716%)

correlation matrix of the fit parameters:

	a	b	c
a	1.000		
b	-0.934	1.000	
c	0.841	-0.974	1.000

Wed Nov 5 11:18:56 2003

FIT: data read from "LACF_FOM_M13.dat"
#datapoints = 255
residuals are weighted equally (unit weight)

function used for fitting: $f(x) = a + b*x + c*x**2$
fitted parameters initialized with current variable values

Iteration 0

WSSR : 0.185063 delta(WSSR)/WSSR : 0
delta(WSSR) : 0 limit for stopping : 1e-05
lambda : 107.382

initial set of free parameter values

a = 0.543209
b = -0.0529725
c = 0.00128236

After 5 iterations the fit converged.
final sum of squares of residuals : 0.097219
rel. change during last iteration : -2.22573e-10

degrees of freedom (ndf) : 252
rms of residuals (stdfit) = $\sqrt{\text{WSSR}/\text{ndf}}$: 0.0196415
variance of residuals (reduced chisquare) = WSSR/ndf : 0.00038579

Final set of parameters	Asymptotic Standard Error
=====	=====
a = 0.556172	+/- 0.006324 (1.137%)
b = -0.0496248	+/- 0.0012 (2.419%)
c = 0.00105159	+/- 5.324e-05 (5.063%)

correlation matrix of the fit parameters:

	a	b	c
a	1.000		
b	-0.934	1.000	
c	0.841	-0.974	1.000

Wed Nov 5 11:21:18 2003

FIT: data read from "LACF_FOM_M14.dat"
#datapoints = 255
residuals are weighted equally (unit weight)

function used for fitting: $f(x) = a + b*x + c*x**2$
fitted parameters initialized with current variable values

Iteration 0

WSSR : 0.120431 delta(WSSR)/WSSR : 0
delta(WSSR) : 0 limit for stopping : 1e-05
lambda : 107.382

initial set of free parameter values

a = 0.556172
b = -0.0496248
c = 0.00105159

After 5 iterations the fit converged.
final sum of squares of residuals : 0.113985
rel. change during last iteration : -7.1941e-10

degrees of freedom (ndf) : 252
rms of residuals (stdfit) = $\sqrt{\text{WSSR}/\text{ndf}}$: 0.0212679
variance of residuals (reduced chisquare) = WSSR/ndf : 0.000452321

Final set of parameters		Asymptotic Standard Error	
=====		=====	
a	= 0.532712	+/- 0.006848	(1.285%)
b	= -0.0461978	+/- 0.0013	(2.813%)
c	= 0.000932419	+/- 5.765e-05	(6.183%)

correlation matrix of the fit parameters:

	a	b	c
a	1.000		
b	-0.934	1.000	
c	0.841	-0.974	1.000

Wed Nov 5 11:22:56 2003

FIT: data read from "LACF_FOM_M15.dat"
#datapoints = 255
residuals are weighted equally (unit weight)

function used for fitting: $f(x) = a + b*x + c*x**2$
fitted parameters initialized with current variable values

Iteration 0

WSSR : 0.134589 delta(WSSR)/WSSR : 0
delta(WSSR) : 0 limit for stopping : 1e-05
lambda : 107.382

initial set of free parameter values

a = 0.532712
b = -0.0461978
c = 0.000932419

After 5 iterations the fit converged.
final sum of squares of residuals : 0.122018
rel. change during last iteration : -2.76716e-10

degrees of freedom (ndf) : 252
rms of residuals (stdfit) = $\sqrt{\text{WSSR}/\text{ndf}}$: 0.0220045
variance of residuals (reduced chisquare) = WSSR/ndf : 0.0004842

Final set of parameters	Asymptotic Standard Error
=====	=====
a = 0.547324	+/- 0.007085 (1.294%)
b = -0.050867	+/- 0.001345 (2.644%)
c = 0.00115905	+/- 5.965e-05 (5.146%)

correlation matrix of the fit parameters:

	a	b	c
a	1.000		
b	-0.934	1.000	
c	0.841	-0.974	1.000

Wed Nov 5 11:25:22 2003

FIT: data read from "LACF_FOM_M16.dat"
#datapoints = 255
residuals are weighted equally (unit weight)

function used for fitting: $f(x) = a + b*x + c*x**2$
fitted parameters initialized with current variable values

Iteration 0

WSSR : 0.168252 delta(WSSR)/WSSR : 0
delta(WSSR) : 0 limit for stopping : 1e-05
lambda : 107.382

initial set of free parameter values

a = 0.547324
b = -0.050867
c = 0.00115905

After 5 iterations the fit converged.
final sum of squares of residuals : 0.119661
rel. change during last iteration : -4.16995e-10

degrees of freedom (ndf) : 252
rms of residuals (stdfit) = $\sqrt{\text{WSSR}/\text{ndf}}$: 0.0217909
variance of residuals (reduced chisquare) = WSSR/ndf : 0.000474844

Final set of parameters	Asymptotic Standard Error
=====	=====
a = 0.566178	+/- 0.007016 (1.239%)
b = -0.0504389	+/- 0.001332 (2.64%)
c = 0.00108757	+/- 5.907e-05 (5.431%)

correlation matrix of the fit parameters:

	a	b	c
a	1.000		
b	-0.934	1.000	
c	0.841	-0.974	1.000

References

- [1] Schonfelder et., al.: 1980, ApJ, 240, 350
- [2] Mandrov et., al.: 1979
- [3] Space Science Reviews 57: 109-186, 1991
- [4] Ables, J.G.: 1968, Proc. Astron. Soc. Australia, 1, 172
- [5] Baumert, L.D.: 1971, "Lecture Notes in Mathematics No. 182: Cyclic Difference Sets" (Berlin:Springer)
- [6] Caroli, E., Stephen, J.B., Di Cocco, G., Natalucci, L., Spizzichino, A.: 1987, Space Sci. Rev., 45, 349
- [7] Fenimore, E.E., Cannon, T.M.: 1978, Appl. Opt., 17, 337
- [8] in 't Zand, J.J.M.: 1992, "A Coded-Mask Imager as monitor of Galactic X-ray Sources", Ph.D. Thesis, Utrecht University
- [9] Peterson, W.W.: 1961, "Error Correcting Codes" (Massachusetts: MIT press)